



# Ultralight scalar field dark matter in modified gravity theories

Aoki, Arata

---

(Degree)

博士 (理学)

(Date of Degree)

2019-03-25

(Date of Publication)

2020-03-01

(Resource Type)

doctoral thesis

(Report Number)

甲第7434号

(URL)

<https://hdl.handle.net/20.500.14094/D1007434>

※ 当コンテンツは神戸大学の学術成果です。無断複製・不正使用等を禁じます。著作権法で認められている範囲内で、適切にご利用ください。



Doctoral Dissertation

Ultralight scalar field dark matter  
in modified gravity theories

(修正重力理論における超軽量スカラー暗黒物質)

January 2019

Graduate School of Science, Kobe University

Arata Aoki

(青木 新)



# Contents

<b>1</b>	<b>Introduction</b>	<b>5</b>
1.1	Overview of Dark Matter and Dark Energy . . . . .	5
1.2	Purpose of Research . . . . .	6
1.3	Outline of Thesis . . . . .	7
1.4	Notations and Definitions . . . . .	8
<b>2</b>	<b>Ultralight Scalar Field Dark Matter</b>	<b>9</b>
2.1	Motivations and Origins . . . . .	9
2.1.1	“Small Scale Crisis” of Cold Dark Matter . . . . .	9
2.1.2	Ultralight Scalar Fields in Particle Theory . . . . .	11
2.2	Properties — Difference from Cold Dark Matter Model . . . . .	12
2.2.1	Homogeneous Background Evolution . . . . .	12
2.2.2	Linear Perturbations and Cosmological Jeans Scale . . . . .	15
2.2.3	Distribution in Galaxies . . . . .	16
2.3	Constraints on Ultralight Scalar Field Dark Matter . . . . .	18
2.3.1	Cosmic Microwave Background . . . . .	19
2.3.2	Ly- $\alpha$ Forest . . . . .	19
2.4	Effect on Gravitational Potentials and Direct Detection Methods . . . . .	20
2.4.1	Gravitational Potential Oscillation Sourced by Oscillating Pressure of Ultralight Scalar Field Dark Matter . . . . .	20
2.4.2	Detection Method I: Pulsar Timing Array Experiments . . . . .	22
2.4.3	Detection Method II: Laser Interferometers . . . . .	24
<b>3</b>	<b>Modified Gravity Theories</b>	<b>29</b>
3.1	Motivations for Alternative Theories of Gravity . . . . .	29
3.2	$f(R)$ Theory . . . . .	30
3.2.1	Overview of $f(R)$ Theory . . . . .	30
3.2.2	Scalar-Tensor Formalism of $f(R)$ Theory . . . . .	31
3.2.3	Relation to Other Modified Gravity Theories . . . . .	33
3.3	Constraints on $f(R)$ Theory . . . . .	34
3.3.1	Local Gravity Constraints . . . . .	34
3.3.2	Cosmological Constraints . . . . .	36
3.3.3	Constraints from Speed of Gravitational Wave . . . . .	37

<b>4</b>	<b>Ultralight Scalar Field Dark Matter in <math>f(R)</math> Theory I: Formalism</b>	<b>38</b>
4.1	Formulation in $f(R)$ Theory . . . . .	38
4.2	Formulation in Scalar-Tensor Theory . . . . .	40
<b>5</b>	<b>Ultralight Scalar Field Dark Matter in <math>f(R)</math> Theory II: Models</b>	<b>43</b>
5.1	Quadratic Model . . . . .	43
5.2	Exponential Model . . . . .	45
5.2.1	Perturbative Approach . . . . .	47
5.2.2	Numerical Approach . . . . .	48
5.2.3	Constraint on Exponential Model . . . . .	50
5.3	Cosmological Dark Energy Models . . . . .	51
5.3.1	Effective Potential of Scalaron Field . . . . .	52
5.3.2	Constraints on Hu-Sawicki/Starobinsky model . . . . .	53
5.3.3	Numerical Approach . . . . .	55
<b>6</b>	<b>Conclusion</b>	<b>57</b>
	<b>Acknowledgement</b>	<b>58</b>
	<b>Reference</b>	<b>61</b>

# Chapter 1

## Introduction

### 1.1 Overview of Dark Matter and Dark Energy

A number of observations have revealed that the energy density of our universe is made up of not only the standard model particles but also unknown dark matter and dark energy. The  $\Lambda$ CDM model is currently believed to be the most plausible cosmological model, where dark energy is assumed to be the cosmological constant (denoted as  $\Lambda$ ) and dark matter is modeled by a slowly-moving pressureless perfect fluid (cold dark matter, CDM). The most accurate probe of the universe is the fluctuations in the cosmic microwave background (CMB) radiation. The observation by the Planck satellite determined the energy density of (cold) dark matter and dark energy (the cosmological constant) as  $\Omega_{\text{CDM}} = 0.264$  and  $\Omega_{\Lambda} = 0.685$ , respectively [1], with assuming the flat  $\Lambda$ CDM model.

Dark matter is originally introduced to explain the so-called “missing mass” in the galaxies, and is also necessary for explaining the distribution of galaxies. Since dark matter is assumed to have no (or extremely tiny) interaction with the standard model particles, it is able to form gravitationally bound objects much earlier than the baryons do. Without (cold) dark matter, the formation of galaxy would not be efficient enough to explain the number of galaxies today. Moreover we can see the distribution of dark matter directly by gravitational lensing observations. For the above reasons, the existence of dark matter is generally accepted.

In the past, the neutrino was considered to be a candidate for dark matter. However, it turned out that the neutrino erases the small scale structure due to its large velocity dispersion, and is not compatible to the observations if all the dark matter density is explained by the neutrino. Hence it is regarded that the neutrino cannot explain all the dark matter density today. At present, a number of scientists are considering that dark matter is made up of unknown particles included in a beyond standard model of the particle theory. A weakly interacting massive particle (WIMP) is an example. A virtue of WIMPs is its ability to explain the present abundance of dark matter naturally, which is known as the “WIMP miracle”. From the point of view of particle theory, supersymmetric extensions of the standard model usually predict WIMPs, e.g. neutralinos. However, there is no experimental signature of supersymmetry so far. Another candidate for dark matter is

the axion (or the QCD axion). It is originally introduced to resolve the so-called “strong CP problem” in the quantum chromodynamics (QCD). The axion is a pseudo-Nambu-Goldstone boson, which arises due to the breaking of a new global chiral U(1) symmetry (the Peccei-Quinn symmetry). The superstring theory also predicts a number of scalar particles, which are called the “string axions” or “axion-like particles.”

We also believe dark energy does exist by mostly three facts. The first is the fluctuations in the CMB as mentioned before. The second is the discovery of the accelerated expansion of the universe today. The observations of the type Ia supernovae revealed that the expansion of the universe is accelerating other than decelerating. In order to explain this fact, we need to assume that a peculiar species with negative pressure dominates the energy density of the present universe. Thirdly, the observations of the baryon acoustic oscillation (BAO) also prefer the existence of dark energy. Combining these facts, it seems inevitable to believe the existence of dark energy.

In the  $\Lambda$ CDM model, dark energy is assumed to be the cosmological constant, which is not forbidden in Einstein’s theory of gravity. In fact, it is well known that Einstein himself introduced the cosmological constant into his theory in order for the universe to be stable. The cosmological constant is the simplest candidate for dark energy. However, there known to be several problems on the cosmological constant. One is the necessity of the fine-tuning of the vacuum energy. From the viewpoint of quantum field theory, the vacuum energy of fields contribute to the cosmological constant. The vacuum energy density  $\rho_{\text{vac}}$  can be estimated as  $\rho_{\text{vac}} \sim M_{\text{Pl}}^4$ , which is larger than the cosmological constant by a factor of  $\mathcal{O}(10^{120})$ . No one can explain this gap naturally. The other problem is known as the coincidence problem. We do not know why the energy density of dark energy today is the same order as that of dark matter. Of course, if the energy density of dark energy were too large, galaxies would not be formed since the accelerated expansion starts earlier. However, such an anthropic principle cannot be applied for the explanation why dark energy is not smaller than the observed value. That is, there would not arise no problem even if dark energy is effectively zero at present time. Given this situation, people are trying to understand these facts by considering alternative possibilities for dark energy. Roughly speaking, there are two possibilities, depending on which term of Einstein’s equation  $G_{\mu\nu} = 8\pi GT_{\mu\nu}$  to be modified. One way is introducing a new species with an equation of state  $w \simeq -1$  into the right-hand-side of Einstein’s equation. This new field is called quintessence, which is usually assumed to be a scalar field that rolls slowly on its potential. The potential energy of quintessence causes the accelerated expansion of the universe as in the case of inflation. Another way is modifying the left-hand-side of Einstein’s equation, that is, modifying Einstein’s theory of general relativity on cosmological scale.

## 1.2 Purpose of Research

As explained in the previous section, dark matter and dark energy are the most serious problems in cosmology. In most researches on these dark components in the universe, people study them separately. That is, dark energy tends to be neglected or assumed to be the cosmological constant when studying dark matter. On the other hand, when studying

dark energy models, cold dark matter is usually assumed (sometimes implicitly). Thus it might be worth investigating dark matter and dark energy models simultaneously if it arises nontrivial phenomena by doing so.

In the previous study by Khmelnitsky and Rubakov [2], they revealed that there is an interesting gravitational phenomenon caused by ultralight scalar field dark matter. As explained in Sec. 2.4, the oscillating pressure of ultralight scalar field dark matter induces the oscillation of the gravitational potentials. This phenomenon is remarkable in the sense that it could be observed by future gravitational experiments. This study is based on Einstein's theory as usual. Thus it is worth reinvestigating this phenomenon in the framework of other gravity theories. Hence the purpose of this research is to study how the phenomenon caused by ultralight scalar field dark matter changes when considering alternative theories of gravity.

### 1.3 Outline of Thesis

This thesis is organized as follows:

- In Chap. 2, the ultralight scalar field dark matter model is reviewed. In Sec. 2.1 motivations for ultralight scalar field dark matter and its possible origins in particle theory are explained. We see some properties of ultralight scalar field dark matter in Sec. 2.2, where we especially focus on differences from the standard cold dark matter model. The existing constraints on ultralight scalar field dark matter are summarized in Sec. 2.3. In Sec. 2.4 we discuss a phenomenon that the gravitational potential is forced to oscillate because of the presence of the oscillating pressure of ultralight scalar field dark matter. We also introduce direct detection methods for this oscillating gravitational potential there.
- In Chap. 3, modified gravity theories are reviewed. In Sec. 3.1 motivations for alternative theories of gravity are explained. We focus on the  $f(R)$  theory as a simple example of modified gravity theories in Sec. 3.2. The equivalence of the  $f(R)$  theory and the scalar-tensor theory is explained, and the relation to other modified gravity theories is discussed in this section. In Sec. 3.3 constraints on the  $f(R)$  models are summarized.
- Chap. 4 and Chap. 5 are the main parts of the thesis, where the behavior of ultralight scalar field dark matter in the  $f(R)$  theory is studied. In Sec. 4.1 we derive the formula for calculating the oscillating part of the gravitational potential in the  $f(R)$  theory. Then we move onto the scalar-tensor formalism of the  $f(R)$  theory, in which we can easily understand the physics, in Sec. 4.2. In Chap. 5, we study specific  $f(R)$  models in order: the quadratic model  $f(R) \propto R^2$ , the exponential model  $f(R) \sim \exp(-R)$ , and the cosmological dark energy models known as the Hu-Sawicki and Starobinsky model.
- Chap. 6 is devoted to the conclusion.

## 1.4 Notations and Definitions

- The signature of the metric tensor is  $(-, +, +, +)$ . That is, the metric of the 4-dimensional flat spacetime is  $\eta_{\mu\nu} = \text{diag}(-1, 1, 1, 1)$ .
- The natural unit  $c = \hbar = 8\pi G = 1$  is used.
- The quantities related to the differential geometry are defined as follows:

- Christoffel symbol

$$\Gamma_{\mu\nu}^{\lambda} = \frac{1}{2}g^{\lambda\alpha}(g_{\alpha\mu,\nu} + g_{\alpha\nu,\mu} - g_{\mu\nu,\alpha}) . \quad (1.4.1)$$

- Riemann tensor

$$R^{\mu}{}_{\nu\rho\sigma} = \Gamma_{\nu\sigma,\rho}^{\mu} - \Gamma_{\nu\rho,\sigma}^{\mu} + \Gamma_{\alpha\rho}^{\mu}\Gamma_{\nu\sigma}^{\alpha} - \Gamma_{\alpha\sigma}^{\mu}\Gamma_{\nu\rho}^{\alpha} . \quad (1.4.2)$$

- Ricci tensor

$$R_{\mu\nu} = R^{\alpha}{}_{\mu\alpha\nu} = \Gamma_{\mu\alpha,\nu}^{\alpha} - \Gamma_{\mu\nu,\alpha}^{\alpha} + \Gamma_{\beta\nu}^{\alpha}\Gamma_{\mu\alpha}^{\beta} - \Gamma_{\beta\alpha}^{\alpha}\Gamma_{\mu\nu}^{\beta} . \quad (1.4.3)$$

- Ricci scalar

$$R = g^{\mu\nu}R_{\mu\nu} = R^{\alpha}{}_{\alpha} . \quad (1.4.4)$$

- Einstein tensor

$$G_{\mu\nu} = R_{\mu\nu} - \frac{1}{2}g_{\mu\nu}R . \quad (1.4.5)$$

# Chapter 2

## Ultralight Scalar Field Dark Matter

In this chapter, the ultralight scalar field dark matter model is reviewed. In Sec. 2.1 motivations for ultralight scalar field dark matter and its possible origins in particle theory are explained. We see some properties of ultralight scalar field dark matter in Sec. 2.2, where we especially focus on differences from the standard cold dark matter model. The existing constraints on ultralight scalar field dark matter are summarized in Sec. 2.3. In Sec. 2.4 we discuss a phenomenon that the gravitational potential is forced to oscillate because of the presence of the oscillating pressure of ultralight scalar field dark matter. We also introduce direct detection methods for this oscillating gravitational potential there.

For more details of the ultralight scalar field dark matter model not covered in this chapter, see review papers Ref. 3 and Ref. 4.

### 2.1 Motivations and Origins

In this section we explain some motivations for ultralight scalar field dark matter, and show its possible origins in particle theory. In Subsec. 2.1.1 we review the so-called “small scale crisis” of cold dark matter, which is the original motivation for considering ultralight scalar field dark matter. In Subsec. 2.1.2 we explain how the ultralight scalar field arises in particle theory.

#### 2.1.1 “Small Scale Crisis” of Cold Dark Matter

In order to explain cosmological scale observations such as the cosmic microwave background anisotropy and the large scale structure of the universe, dark matter must be *cold*. That is, the motion of dark matter particles must be slow compared to the speed of light so that its pressure is sufficiently small. However it is known that there are some tensions between the predictions of the cold dark matter model and galactic scale observations. In fact, the necessity of the pressureless nature of dark matter is essentially from cosmological scale or larger-than-galactic scale observations. Hence there is no reason to believe that the pressureless nature of cold dark matter should hold on small scales. These tensions between the theoretical prediction and the observations are often referred to as the “small

scale crisis” of cold dark matter [5]. Some examples of them are the cusp-core problem, the missing satellites problem, and the too-big-to-fail problem. All the problems are essentially related to overabundance of structure on small scales in the cold dark matter model, which is due to the pressureless nature of cold dark matter. Thus in order to resolve these issues, we need a mechanism to relax the overabundance of dark matter distribution in galaxies.

The solution could lie in baryonic physics that are not modeled adequately: Some numerical simulations claim that feedback from astrophysical processes such as supernovae or star formation can flatten the central cusps of halos in massive galaxies. On the other hand, the crisis might be resolved by nature of dark matter. Some proposals are the self-interacting dark matter model, the warm dark matter model, or the ultralight scalar field dark matter model [6]. In the self-interacting dark matter model, people try to erase the overabundance of dark matter by the pressure due to its self-interaction, with a cross section of order  $\sigma/m \gtrsim 1 \text{ cm}^2/\text{g}$ . In the warm dark matter model, a thermally-produced particle with a keV-scale mass is assumed. Its free-streaming scale, the distance a particle can travel over in one Hubble time  $H^{-1}$ , is roughly corresponding to galactic scale. Warm dark matter erases structure smaller than its free-streaming scale.

The ultralight scalar field dark matter model is another possible solution to the small scale tensions. In this model we assume a non-thermally produced scalar particles with extremely small mass. Scalar particles behave as classical wave due to its bosonic nature (c.f. electromagnetic wave) if its occupation number is sufficiently large. Thus, according to the uncertainty principle in the (classical) wave mechanics, there arises an effective pressure. The scale at which the effective pressure becomes effective is called the Jeans scale, and as we derive in Sec. 2.2 the (galactic) Jeans scale  $k_J$  is evaluated as

$$k_J \sim \frac{2\pi}{4 \text{ kpc}} \left( \frac{m}{10^{-22} \text{ eV}} \right)^{1/2}, \quad (2.1.1)$$

where  $m$  is the mass of the scalar field. Hence the effective pressure becomes important at galactic scale ( $\sim 10 \text{ kpc}$ ) if the mass of the scalar field is around  $10^{-22} \text{ eV}$ . The structure below the Jeans scale is erased, as qualitatively similar to the warm dark matter model. For this reason, ultralight scalar field dark matter is often called “fuzzy dark matter” [6]. Strictly speaking, fuzzy dark matter is often defined as the limiting case of ultralight scalar field dark matter with negligible self-interaction. This is the original motivation to expect the ultralight scalar field as a dark matter candidate.

We should note that both the model predictions and the observations tend to have considerable ambiguities: The theoretical predictions are based on numerical simulations of complex nonlinear system including baryonic species, and there should be systematic numerical errors that is difficult to evaluate correctly. The observations on galactic scale always have a number of statistical and systematic errors. Hence there are discussions whether the “small scale crisis” is indeed the problem.

In this thesis we do not care the “small scale crisis” and not require the mass of the scalar field to be around  $m \sim 10^{-22} \text{ eV}$ . We use this value just for reference.

### 2.1.2 Ultralight Scalar Fields in Particle Theory

In this subsection we review possible origins of ultralight scalar fields in particle theory. This subsection is mostly based on Sec. II of Ref. 4.

Scalar fields often appear in particles theories that beyond the standard model. If the action for a scalar field  $\phi$  has the shift symmetry  $\phi \rightarrow \phi + C$ , the mass term  $(1/2)m^2\phi^2$  is forbidden. In other words, the shift symmetry is broken by adding the mass term or general self-interaction  $V(\phi)$ . The shift symmetry is a continuous and global symmetry. However, all the continuous global symmetries are considered to be broken in quantum gravity. Thus we believe that the shift symmetry of the scalar field is only approximate one, and the scalar field should have a small mass. Such a situation naturally arises when the scalar field is an angular variable. The so-called axionlike particles predicted in some extensions of the standard model, especially in string theory, are examples of them. We can model an axionlike particle as

$$S = \int d^4x \sqrt{-g} \left[ \frac{1}{2}(\partial\phi)^2 - \mu^4 [1 - \cos(\phi/F)] \right], \quad (2.1.2)$$

where  $\mu$  and  $F$  are parameters to be discussed later. The continuous shift symmetry is broken into the discrete one,  $\phi \rightarrow \phi + 2\pi F$ , because of the presence of the potential term, which usually generated by nonperturbative instanton effect. By expanding the potential, the mass of the field is identified as

$$m = \frac{\mu^2}{F}. \quad (2.1.3)$$

The parameter  $F$ , which is often called the decay constant, is assumed to be within the Planck scale  $M_{\text{Pl}} \equiv 1/\sqrt{8\pi G} = 2.4 \times 10^{18}$  GeV and the so-called grand unification energy scale  $M_{\text{GUT}} \sim 10^{16}$ :

$$10^{16} \text{ GeV} \lesssim F \lesssim 10^{18} \text{ GeV}. \quad (2.1.4)$$

Another parameter  $\mu$  is generated by the nonperturbative instanton effect, and roughly estimated as  $\mu^4 \sim M_{\text{Pl}}^2 \Lambda^2 e^{-\sigma}$ , where  $\sigma$  is the instant action and  $\Lambda$  measures a possible suppression of instanton effects due to supersymmetry. The value of  $\Lambda$  depends on models and its range is assumed to be  $10^4 \text{ GeV} \lesssim \Lambda \lesssim 10^{18} \text{ GeV}$ . The instanton action  $\sigma$  also depends on models. In some simple cases we can assume  $\sigma \sim \sigma_0 = 2\pi/\alpha_G$ , where  $\alpha_G$  is the standard model gauge coupling extrapolated to the grand unification energy scale. If we use a value  $\alpha_G = 1/25$ , which is based on the assumption that only known particles in the standard model contribute to  $\alpha_G$ , the possible mass range of the scalar field is evaluated as

$$10^{-21} \text{ eV} \lesssim m \lesssim 10^{-5} \text{ eV}. \quad (2.1.5)$$

If we use  $\alpha_G = 1/30$  instead, the range is

$$10^{-28} \text{ eV} \lesssim m \lesssim 10^{-12} \text{ eV}. \quad (2.1.6)$$

Since the mass depends exponentially on the action  $\sigma$ , we cannot make a strict prediction by this estimation. One point we would like to stress is that the mass in question ( $m \sim 10^{-22}$  eV) could naturally arise in particle theory beyond the standard model.

In this subsection we have seen how ultralight scalar fields arise in particle theory and discussed an axionlike particle as a concrete example. It should be noted that it is not crucial that an ultralight scalar field is an axionlike particle for the purpose of this thesis. All the assumptions in the thesis are its bosonic nature and negligible (self-)interactions.

## 2.2 Properties — Difference from Cold Dark Matter Model

In Subsec. 2.1.1 we mentioned that ultralight scalar field dark matter behaves differently from cold dark matter below the Jeans scale, which is determined by its mass. In this section we see such properties more quantitatively by studying its behavior in cosmological and astrophysical situations.

Let us consider a theory of a free scalar field  $\phi(t, \mathbf{x})$  defined by the action

$$S = \int d^4x \sqrt{-g} \left[ \frac{1}{2} (\partial\phi)^2 - \frac{1}{2} m^2 \phi^2 \right] , \quad (2.2.1)$$

where  $m$  is the mass. We assume that the background universe is homogeneous, isotropic, and spatially flat. Such an universe is realized by the flat Friedmann-Lemaître-Robertson-Walker metric:

$$ds^2 = -dt^2 + a(t)^2 d\mathbf{x}^2 . \quad (2.2.2)$$

where  $a(t)$  is the scale factor normalized as  $a = 1$  today,  $t$  is the cosmic time, and  $\mathbf{x}$  is the comoving coordinate.

We then separate the scalar field  $\phi(t, \mathbf{x})$  into the homogeneous background part  $\bar{\phi}(t)$  and the small fluctuation  $\delta\phi(t, \mathbf{x})$ , i.e.,  $\phi(t, \mathbf{x}) = \bar{\phi}(t) + \delta\phi(t, \mathbf{x})$ . In Subsec. 2.2.1 we study the homogeneous background field  $\bar{\phi}$  and confirm that it indeed behaves in the same way as cold dark matter on cosmological scale. Then, we study the behavior of the perturbed field  $\delta\phi$  in Subsec. 2.2.2, where the (cosmological) Jeans scale is derived. In Subsec. 2.2.3 we discuss the galactic scale behavior of ultralight scalar field dark matter.

### 2.2.1 Homogeneous Background Evolution

In this subsection we omit the bar symbol of  $\bar{\phi}$  and write the background field as  $\phi$  for simplicity. The scalar field obeys the Klein-Gordon equation, and in the expanding universe it is written as

$$\ddot{\phi} + 3H\dot{\phi} + m^2\phi = 0 , \quad (2.2.3)$$

where  $H \equiv \dot{a}/a$  is the Hubble parameter and the dot denotes the derivative with respect to the cosmic time  $t$ . The solutions to Eq. (2.2.3) behave differently in early time ( $H \gg m$ ) and late time ( $H \ll m$ ).

In the early universe ( $H \gg m$ ), the dominant solution is just a constant,  $\phi = \text{Const.}$  Note that another independent solution decays in proportion to  $a^{-3}$  with the expansion of the universe. The kinetic energy of the field is extremely small since the field is frozen to a

constant value. Hence the energy density  $\rho$  is almost a constant and the pressure is  $p \simeq -\rho$ . Thus the field has a dark energy-like equation of state,  $w = p/\rho \simeq -1$ .

The field starts to oscillate at the bottom of the potential when it becomes  $H \sim m$ . During this period, the solution can be written by using the WKB approximation as

$$\phi(t) = \phi_0 a^{-3/2} \cos(mt + \alpha) , \quad (2.2.4)$$

where  $\phi_0$  and  $\alpha$  are constants. Note that the constant  $\phi_0$  is the amplitude at the present time. The energy density of the scalar field is

$$\rho = \frac{1}{2}\dot{\phi}^2 + \frac{1}{2}m^2\phi^2 = \frac{1}{2}m^2\phi_0^2 a^{-3} + \mathcal{O}(H/m) , \quad (2.2.5)$$

where  $\mathcal{O}(H/m)$  is an oscillating correction term. With ignoring the correction term, the energy density decays proportional to  $a^{-3}$  as the case of the cold dark matter fluid. Hence the larger the mass is, the more the scalar field dark matter mimics cold dark matter on cosmological scale. The pressure of the field is

$$p = \frac{1}{2}\dot{\phi}^2 - \frac{1}{2}m^2\phi^2 = -\rho \cos(2mt + 2\alpha) + \mathcal{O}(H/m) . \quad (2.2.6)$$

Thus the pressure oscillates in time with angular  $\omega = 2m$ , and its amplitude is fixed by the energy density  $\rho$ . The pressure is a rapidly oscillating function since the period of the oscillation  $T \sim m^{-1}$  is much shorter than the cosmological time scale,  $H^{-1}$ . Hence the oscillating pressure has almost no effect on the cosmological expansion of the universe despite its amplitude being not small. We can confirm this explicitly by numerical calculation.

The evolution of the energy is plotted in Fig. 2.1 for  $m = 10^{-25}$  eV, which is obtained by simultaneously solving the Friedmann equation, the Klein-Gordon equation for the scalar field, and the equations of state for other species. The scale factor at the beginning of the oscillation  $a_{\text{osc}}$  is defined by the condition  $3H(a_{\text{osc}}) = m$ . After the time  $a \sim a_{\text{osc}}$ , the energy density of the scalar field decays proportional to  $a^{-3}$  as the case of the cold dark matter fluid. Since the field starts to oscillate in the radiation dominant era, the Hubble parameter at  $a = a_{\text{osc}}$  can be estimated as

$$H_{\text{osc}} \simeq H_{\text{eq}} \left( \frac{a_{\text{eq}}}{a_{\text{osc}}} \right)^2 = \frac{H_0 a_{\text{eq}}^{1/2}}{a_{\text{osc}}^2} , \quad (2.2.7)$$

where  $H_{\text{eq}} \simeq H_0 a_{\text{eq}}^{-3/2}$  is the Hubble parameter at the equal time ( $\rho_r = \rho_b + \rho_\phi$ ). Hence  $a_{\text{osc}}$  is evaluated as

$$a_{\text{osc}} \simeq \sqrt{\frac{3H_0}{m}} a_{\text{eq}}^{1/4} = 8.6 \times 10^{-7} \left( \frac{m}{10^{-22} \text{ eV}} \right)^{-1/2} . \quad (2.2.8)$$

where we used  $a_{\text{eq}} = 1/3400$  and  $H_0 = 67.31$  km/s/Mpc.

For numerical calculations we need the initial value of the field  $\phi_i$ . We use the shooting method, in which  $\phi_i$  is adjusted so that the present value of the energy density  $\rho_\phi/\rho_{\text{cr}}$  matches an input value  $\Omega_\phi$ . The rough estimation for  $\phi_i$  is given as follows. Since the

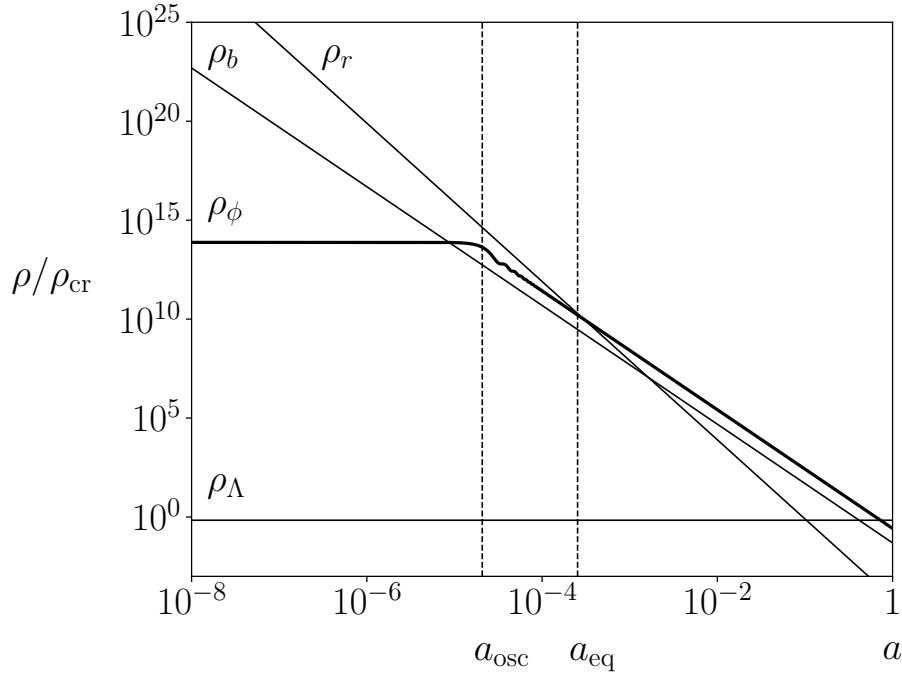


Figure 2.1: The evolution of the energy density of radiation ( $\rho_r$ ), baryon ( $\rho_b$ ), cosmological constant ( $\rho_\Lambda$ ), and ultralight scalar field dark matter ( $\rho_\phi$ ), normalized by the critical density  $\rho_{\text{cr}}$ . The scalar field starts to oscillate at  $a \sim a_{\text{osc}}$ , which is determined by the condition  $3H(a_{\text{osc}}) = m$ . The scale factor at radiation-matter equality ( $\rho_r = \rho_b + \rho_\phi$ ) is indicated as  $a_{\text{eq}}$ . The mass of the scalar field is chosen to be  $m = 10^{-25}$  eV.

field starts to oscillate at  $a = a_{\text{osc}}$  and then the field decays proportional to  $a^{-3/2}$ ,  $\phi_i$  is approximated as

$$\phi_i \simeq a_{\text{osc}}^{-3/2} \phi_0 \simeq 0.023 \left( \frac{m}{10^{-22} \text{ eV}} \right)^{-1/4}, \quad (2.2.9)$$

where we used the fact  $(1/2)m^2\phi_0^2 = \Omega_\phi\rho_{\text{cr}}$  and the value  $\Omega_\phi h^2 = 0.1197$ . Thus for the mass  $m = 10^{-22}$  eV the initial value of the field is  $\phi_i \sim 10^{-2} M_{\text{Pl}} \sim 10^{16}$  GeV. If we assume the scalar field as an axionlike particle, a natural value for  $\phi_i$  is  $\phi_i \sim F$ , where  $F$  is the decay constant. Hence we have an interesting fact that a parameter set  $(m, F) \sim (10^{-22} \text{ eV}, 10^{16} \text{ GeV})$  naturally predict the desired value for the energy density.

Clearly we need the condition  $a_{\text{osc}} \ll a_{\text{eq}}$  in order not to spoil the success of the standard  $\Lambda$ CDM cosmology. If we have the condition  $a_{\text{osc}} \gtrsim a_{\text{eq}}$  and fix the energy density at the present time, the equal time  $a_{\text{eq}}$  is changed too much, which leads to the discrepancies with the observations. The Hubble parameter at the radiation-matter equality ( $a = a_{\text{eq}} \simeq 1/3400$ ) is about  $H_{\text{eq}} \sim 10^{-27}$  eV. Hence, the mass of the scalar field must be much larger than  $10^{-27}$  eV. As we will see in Subsec. 2.3.1, the condition for the mass becomes more severe when considering the linear perturbation.

## 2.2.2 Linear Perturbations and Cosmological Jeans Scale

In this subsection we study the behavior of the perturbation  $\delta\phi$  and derive the cosmological Jeans scale. Since the background universe has a translation symmetry, it is convenient to study the Fourier modes  $\delta\phi(t, \mathbf{k})$  instead of  $\delta\phi(t, \mathbf{x})$ . Hereafter we denote  $\delta\tilde{\phi}(t, \mathbf{k})$  simply as  $\delta\phi(t, \mathbf{k})$ . The equation of motion for  $\delta\phi$  is

$$\delta\ddot{\phi} + 3H\delta\dot{\phi} + \left(m^2 + \frac{k^2}{a^2}\right)\delta\phi = \dot{\phi}(\kappa + \dot{A}) + (2\ddot{\phi} + 2H\dot{\phi})A, \quad (2.2.10)$$

where  $\phi$  is the background field,  $A$  is the time-time component of the metric perturbation, and  $\kappa$  is a combination of the metric perturbations [7]. Introducing the fluid variables as usual manner and averaging the variables over the time longer than the period of the oscillation with an appropriate gauge fixing, we obtain the equation for the density contrast  $\delta \equiv \delta\rho/\rho$  as

$$\ddot{\delta} + 2H\dot{\delta} - \left(4\pi G\rho - \frac{k^2}{a^2}c_s^2\right)\delta = 0, \quad (2.2.11)$$

where  $c_s$  is the effective sound speed of the scalar field:

$$c_s^2 \equiv \frac{\delta p}{\delta\rho} = \left[1 + \left(\frac{2ma}{k}\right)^2\right]^{-1}. \quad (2.2.12)$$

This procedure is called the effective fluid approximation for ultralight scalar field dark matter. We have a term  $(k/a)^2c_s^2\delta$  in Eq. (2.2.11), which is absent from the equation for  $\delta$  in the cold dark matter model. This term is often called the “effective pressure” and causes difference between ultralight scalar field dark matter and cold dark matter. The asymptotic forms of the sound speed on small and large scales are

$$c_s \simeq \begin{cases} \frac{k}{2ma} & (k/2ma \ll 1) \\ 1 - \frac{1}{2}\left(\frac{2ma}{k}\right)^2 & (k/2ma \gg 1) \end{cases}. \quad (2.2.13)$$

Hence the evolution of the perturbations depends on scales, which would be a distinguishable feature compared to cold dark matter. For the nonrelativistic perturbations,  $k \ll ma$ , the equation for  $\delta$  becomes

$$\ddot{\delta} + 2H\dot{\delta} - \left(4\pi G\rho - \frac{k^4}{4m^2a^4}\right)\delta = 0. \quad (2.2.14)$$

For large scales ( $k/2ma \ll 1$ ), the effective pressure is negligible and the perturbations behave in the same way as in the cold dark matter model as expected. For smaller scales the effective pressure term becomes important. The scale at which the two terms in the parenthesis in Eq. (2.2.14) are equal to each other is called the (cosmological) Jeans scale  $k_J$ :

$$k_J = (16\pi G\rho m^2 a^4)^{1/4} = \frac{2\pi}{98 \text{ kpc}} a^{1/4} \left(\frac{\Omega_\phi h^2}{0.12}\right)^{1/4} \left(\frac{m}{10^{-22} \text{ eV}}\right)^{1/2}, \quad (2.2.15)$$

where we assumed all the dark matter is ultra-light scalar field dark matter, i.e.,  $\rho = \Omega_\phi \rho_{\text{cr}}$ . Note that as we will see in the next subsection the Jeans scale on galactic scale is an order of magnitude smaller than the cosmological Jeans scale (2.2.15) since the galactic energy density is larger than the cosmological one by about five order of magnitude.

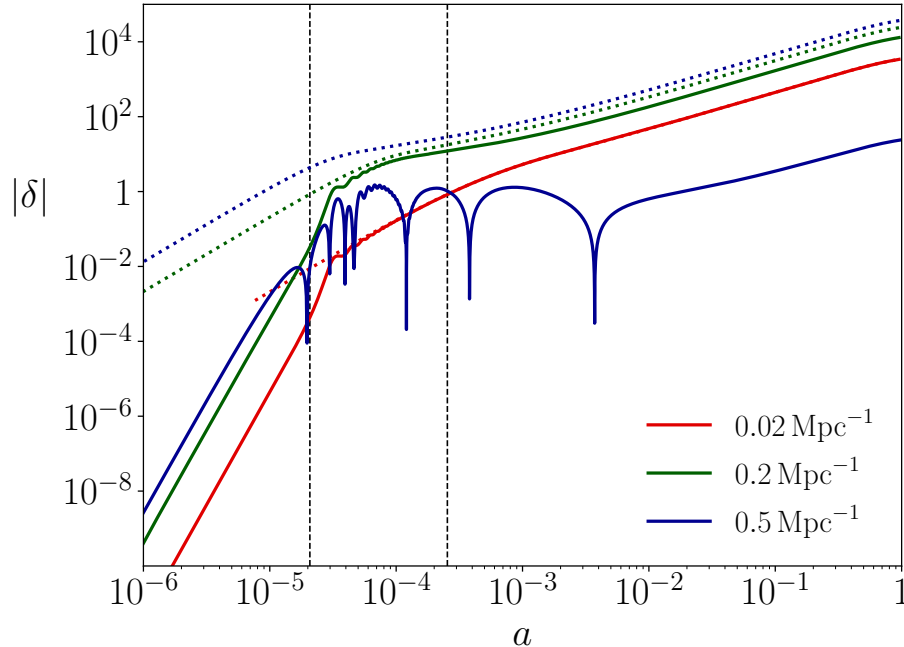


Figure 2.2: The evolution of the density contrast  $\delta$  as a function of the scale factor  $a$ . The solid lines are for the ultra-light scalar field dark matter model and the dashed lines are for the cold dark matter model. The mass of the scalar field is arbitrarily chosen to be  $m = 10^{-25}$  eV for visualization.

In Fig. 2.2 we plot the evolution of the density contrast of dark matter for three different scales.<sup>1</sup> The mass is arbitrarily chosen to be  $m = 10^{-25}$  eV, for which the corresponding cosmological Jeans scale is about 1 Mpc [see Eq. (2.3.1)]. We also plot the density contrast in the standard  $\Lambda$ CDM model for comparison. The largest scale perturbations (red) are indistinguishable from each other, while the smaller scale perturbations (green and blue) in the ultra-light scalar field dark matter model are suppressed relative to that in the cold dark matter model.

### 2.2.3 Distribution in Galaxies

In this subsection we study the galactic scale behavior of ultra-light scalar field dark matter. On galactic scale we cannot rely on the perturbative approach since the nonlinearity of

<sup>1</sup> The numerical calculations are performed by using a public code CLASS [8] with some modifications for ultra-light scalar field dark matter introduced by Ref. 9.

the dynamics becomes important. Since we assume the mass of the scalar field is  $m \gtrsim 10^{-22} \text{ eV} \sim (0.1 \text{ pc})^{-1}$ , we can use the nonrelativistic approximation  $k \ll m$  in analyzing the galactic scale dynamics. As is well known, the Klein-Gordon equation reduces to the Schrödinger-Poisson equation in this situation. We further rewrite the Schrödinger-Poisson equation into the Madelung equations, with which we can see the qualitative difference of ultralight scalar field dark matter from cold dark matter.

A scalar field  $\phi$  satisfies the Klein-Gordon equation

$$(\square - m^2)\phi = 0 . \quad (2.2.16)$$

We can treat the gravitational potentials as perturbations even on small scales since  $\Phi \sim \rho/k^2 \sim 10^{-6}$  for  $\rho = 0.3 \text{ GeV/cm}^3$  and  $k = (10 \text{ kpc})^{-1}$ . The expansion of the universe can be neglected on galactic scale, and we use the Newtonian gauge for the metric:

$$g_{\mu\nu} = \begin{pmatrix} -1 - 2\Psi & 0 \\ 0 & (1 - 2\Phi)\delta_{ij} \end{pmatrix} . \quad (2.2.17)$$

Since we can ignore the anisotropic stress at the leading order, we can set  $\Psi = \Phi$ . Let us introduce a complex scalar field  $\psi$  by

$$\phi = \frac{1}{\sqrt{2m}}(\psi e^{-imt} + \psi^* e^{imt}) , \quad (2.2.18)$$

where  $\psi$  is normalized so that  $|\psi|^2$  has the dimension of energy density. Substituting this into the Klein-Gordon equation and using the nonrelativistic (slow motion) approximation  $m|\dot{\psi}| \gg |\ddot{\psi}|$ ,  $m|\Psi| \gg |\dot{\Psi}|$ , we obtain the Schrödinger equation

$$i \frac{\partial \psi}{\partial t} = -\frac{\nabla^2}{2m} \psi + m\Phi\psi . \quad (2.2.19)$$

In the nonrelativistic limit, the gravitational potential  $\Phi$  is determined by Poisson's equation

$$\nabla^2 \Phi = \frac{1}{2}(|\psi|^2 - \rho_0) , \quad (2.2.20)$$

where  $\rho_0$  is the background energy density that contributes to the homogeneous expansion of the universe and thus subtracted here. Hence, in the nonrelativistic limit the self-gravitating system of the scalar field can be described by the Schrödinger-Poisson equation.

We further rewrite the Schrödinger-Poisson equation by introducing the fluid variables, the energy density  $\rho$  and the velocity  $\mathbf{v}$ . With writing  $\psi = |\psi|e^{i\theta}$ , the fluid variables  $\rho$  and  $\mathbf{v}$  are defined as

$$\rho = |\psi|^2 , \quad \mathbf{v} \equiv \frac{\nabla \theta}{m} . \quad (2.2.21)$$

Then the Schrödinger equation (2.2.19) can be rewritten as the following set of equations:

$$\dot{\rho} + \nabla \cdot (\rho \mathbf{v}) = 0 , \quad (2.2.22)$$

$$\dot{\mathbf{v}} + (\mathbf{v} \cdot \nabla) \mathbf{v} = -\nabla \Phi + \frac{1}{2m^2} \nabla \left( \frac{\nabla^2 \sqrt{\rho}}{\sqrt{\rho}} \right) . \quad (2.2.23)$$

Clearly, the first one is the continuity equation and the second one is the Euler equation with an extra contribution in the right-hand side. These equations are known as the Madelung equations. The quantity

$$\Phi_{\text{QP}} \equiv -\frac{1}{2m^2} \left( \frac{\nabla^2 \sqrt{\rho}}{\sqrt{\rho}} \right), \quad (2.2.24)$$

is sometimes called “quantum pressure” or “quantum potential” by historical reasons while it is not quantum effect. The quantum pressure is absent in the cold dark matter model, and thus it characterizes the difference between ultralight scalar field dark matter and cold dark matter. Since  $\Phi_{\text{QP}}$  is proportional to  $\nabla^2 \sqrt{\rho}$ , it becomes important on small scale. Let us estimate the scale at which the quantum pressure becomes important. For this purpose, let us write the energy density as  $\rho = \rho_0(1 + \delta)$  and assume  $|\delta| \ll 1$  for simplicity, while we consider the nonlinear dynamics. Then the quantum pressure can be approximated as

$$\Phi_{\text{QP}} \simeq -\frac{1}{4m^2} \nabla^2 \delta. \quad (2.2.25)$$

With this assumption, the Madelung equations and Poisson’s equation give

$$\ddot{\delta} - \left( \frac{1}{2}\rho_0 - \frac{k^4}{4m^2} \right) \delta = 0, \quad (2.2.26)$$

where  $|\mathbf{v}| \ll 1$  is assumed, and  $\nabla^2$  is replaced by  $-k^2$ . This is the same as Eq. (2.2.14) with setting  $a = 1$  and replacing  $\rho$  by  $\rho_0$  as desired. Hence we can define the galactic Jeans scale as

$$k_J \equiv (2\rho_0 m^2)^{1/4} = (16\pi G\rho_0 m^2)^{1/4} = \frac{2\pi}{4.28 \text{ kpc}} \left( \frac{m}{10^{-22} \text{ eV}} \right)^{1/2}, \quad (2.2.27)$$

where we used  $\rho_0 = 0.3 \text{ GeV/cm}^3$ . The galactic Jeans scale is smaller than the cosmological one by an order of magnitude since the energy density in the galaxy is larger than the cosmological dark matter density by a factor of  $\sim 10^5$ . Note that the Jeans scale becomes smaller in situations with higher energy density such as around the center of the galaxy.

The fluctuations of ultralight scalar field dark matter evolve in the same way as cold dark matter on scales larger than the galactic Jeans scale, and thus grow up by gravitational instability. On the other hand, smaller scale fluctuations cannot grow up due to the presence of the quantum pressure. Hence we expect ultralight scalar field dark matter forms clumps with a size of the galactic Jeans scale in the galaxy. In fact, the formation of such density granules can be seen in numerical simulations [10]. In the simulations, it is also confirmed that there is a solitonic core rather than cuspy density profile at the center of a galaxy.

## 2.3 Constraints on Ultralight Scalar Field Dark Matter

In this section we review the current limits on the mass of ultralight scalar field dark matter. In summary, the ultralight scalar field dark matter model is consistent with all the observed data if the mass satisfies  $m \gtrsim 10^{-22} \text{ eV}$ .

### 2.3.1 Cosmic Microwave Background

As explained in Sec. 2.2, ultralight scalar field dark matter behave differently from cold dark matter on scales smaller than the Jeans scale. If the Jeans scale is sufficiently large, ultralight scalar field dark matter could affect the CMB fluctuations. The Planck satellite measured the anisotropies of the cosmic microwave background with high sensitivity up to the multipole  $\ell \sim 2500$ , which corresponds to an angular scale  $180^\circ/\ell \sim 0.07^\circ \sim 4$  arcmin. The comoving scale corresponding to the multipole  $\ell = 2500$  is about 6 Mpc. Hence we can probe scales larger than this scale by using the CMB data. Since the cosmological Jeans scale is

$$k_J = \frac{2\pi}{3.1 \text{ Mpc}} a^{1/4} \left( \frac{\Omega_\phi h^2}{0.12} \right)^{1/4} \left( \frac{m}{10^{-25} \text{ eV}} \right)^{1/2}, \quad (2.3.1)$$

the CMB data can be used to probe the mass lighter than  $m \sim 10^{-25}$  eV. We note that the Jeans scale depends weakly on the scale factor  $a$ , the change in which is less than one order of magnitude from the equal time  $a_{\text{eq}} \simeq 1/3400$  to the present time  $a = 1$ .

In Ref. 11 the authors claim that the mass of ultralight scalar field dark matter must be  $m \gtrsim 10^{-24}$  eV in order to be consistent with the observed CMB spectra. They performed the Markov chain Monte Carlo (MCMC) analysis of the data released in 2013 by the Planck Collaboration [12]. They used a Boltzmann code `AxionCAMB` [13] for calculating theoretical CMB spectra, in which the effective fluid approximation is used for ultralight scalar field dark matter. Strictly speaking, they did not constrain the mass directly. They considered a mixed dark matter model in which ultralight scalar field dark matter and standard cold dark matter coexist, and constrained the ratio of two dark matter species. They obtained the result that ultralight scalar field dark matter with a mass lighter than  $m \sim 10^{-24}$  eV cannot explain all the dark matter energy density, otherwise there are too much deviation from the observed CMB spectra. Almost the same analysis was done in Ref. 14 using updated data released in 2015 [15], while the result was not so much changed.

### 2.3.2 Ly- $\alpha$ Forest

Currently, the tightest bound on the mass of ultralight scalar field dark matter is given by the observations of the Lyman- $\alpha$  forest. The Lyman- $\alpha$  forest is the absorption lines in the spectra of high-redshift quasars by neutral hydrogen atoms. We can probe the matter power spectrum at redshift  $z = 2-6$  on comoving scales down to about 0.1 Mpc. The constraints were obtained by Ref. 16 and Ref. 17 as  $m \gtrsim 20 \times 10^{-22}$  eV and  $m \gtrsim 23 \times 10^{-22}$  eV, respectively, at  $2\sigma$  confidence level. We should mention that they used standard collisionless N-body simulations for calculating the dynamics of ultralight scalar field dark matter. That is, the nature of ultralight scalar field dark matter is only included in the initial condition. We also mention that there would be large systematic uncertainties on the constraint above since it is difficult to model dynamics of baryons, and thus the constraint should not be taken so seriously. For these reasons, we use a conservative constraint  $m \gtrsim 10^{-22}$  eV in this thesis, and still use the value  $10^{-22}$  eV for reference.

## 2.4 Effect on Gravitational Potentials and Direct Detection Methods

In this section we focus on galactic scale gravitational phenomena caused by ultralight scalar field dark matter. One distinguishable feature of ultralight scalar field dark matter is its oscillating pressure, as discussed in the previous sections. The oscillating pressure induces the oscillation of the gravitational potentials through Einstein's equation. This oscillation can in principle be detected by future gravitational observations. This phenomenon was first pointed out by Khmelnitsky and Rubakov [2]. They also proposed a detection method for the oscillating gravitational potentials using pulsar timing experiments. We proposed that gravitational-wave laser interferometers are also available for this purpose [18].

In Subsec. 2.4.1, we calculate the oscillating gravitational potential induced by ultralight scalar field dark matter. The detection methods using pulsar timing arrays and gravitational-wave laser interferometers are explained in Subsec. 2.4.2 and Subsec. 2.4.3, respectively.

### 2.4.1 Gravitational Potential Oscillation Sourced by Oscillating Pressure of Ultralight Scalar Field Dark Matter

In this subsection we derive the oscillating part of the gravitational potential induced by the oscillating pressure of ultralight scalar field dark matter based on Einstein's theory. This subsection is based on Sec. 2 of Ref. 2 and Sec. II of Ref. 19.

We consider the situation that the energy density in our galactic halo is dominated by ultralight scalar field dark matter. In order to determine the gravitational potential, we use Einstein's equation

$$G_{\mu\nu} = T_{\mu\nu} . \quad (2.4.1)$$

The trace of Einstein's equation gives

$$R = -T , \quad (2.4.2)$$

where  $T \equiv g^{\mu\nu}T_{\mu\nu}$  is the trace of the energy-momentum tensor of ultralight scalar field dark matter. Note that the trace of the Einstein tensor is  $g^{\mu\nu}G_{\mu\nu} = -R$ . In the following we consider both sides of Eq. (2.4.2) in order.

The expansion of the universe is completely negligible on galactic scale. Thus we use the Newtonian gauge for the metric:

$$g_{\mu\nu} = \begin{pmatrix} -1 - 2\Psi & 0 \\ 0 & (1 - 2\Phi)\delta_{ij} \end{pmatrix} . \quad (2.4.3)$$

Since the gravitational potentials are small even in the galactic halo, we can treat them perturbatively. The Ricci scalar can be calculated at the first order of the potentials as

$$R = -6\ddot{\Phi} + 2\nabla^2(2\Phi - \Psi) , \quad (2.4.4)$$

where a dot denotes the derivative with respect to time. This gives the left-hand side of Eq. (2.4.2).

Next we consider the right-hand side of Eq. (2.4.2). The configuration of the ultralight scalar field in the galaxy can be written as a superposition of plane waves with different wavenumbers. As explained in Subsec. (2.2.3), the wavenumber of the ultralight scalar field is assumed to be less than  $k_J$  since smaller scale structures cannot grow up. We can evaluate  $k_J/m = (16\pi G\rho_0/m^2)^{1/4} \sim 10^{-4}$  for  $m = 10^{-22}$  eV, and this ratio becomes smaller for larger masses. Hence there is a hierarchical relation  $k \lesssim k_J \ll m$ , and thus the dispersion relation reads  $\Omega^2 = m^2 + k^2 \simeq m^2$ . Since we have a monochromatic dispersion relation  $\Omega \simeq m$  in the galaxy, the field  $\phi(t, \vec{x})$  can be written as

$$\phi(t, \vec{x}) = \phi_0(\vec{x}) \cos(mt + \alpha(\vec{x})) . \quad (2.4.5)$$

As the field is homogeneous below the Jeans scale, we can assume  $\phi_0$  and  $\alpha$  to be constant locally. Hereafter we set  $\alpha = 0$  for simplicity. The energy density  $\rho$  and the pressure  $p$  of the field are calculated as

$$\rho = \frac{1}{2}\dot{\phi}^2 + \frac{1}{2}m^2\phi^2 = \frac{1}{2}m^2\phi_0^2 \equiv \rho_0 , \quad (2.4.6)$$

$$p = \frac{1}{2}\dot{\phi}^2 - \frac{1}{2}m^2\phi^2 = -\frac{1}{2}m^2\phi_0^2 \cos(2mt) = -\rho_0 \cos(2mt) . \quad (2.4.7)$$

Here we identified the energy density of the field as the local dark matter density,  $\rho_0 \sim 0.3 \text{ GeV/cm}^3$ . Hence the pressure of the scalar field oscillates in time with an angular frequency  $\omega = 2m$ . The amplitude of the pressure is fixed by the local dark matter density. Thus the energy-momentum tensor of ultralight scalar field dark matter in the galaxy can be written as

$$T_{\mu\nu} = \begin{pmatrix} \rho_0 & 0 \\ 0 & -\rho_0 \cos(2mt)\delta_{ij} \end{pmatrix} , \quad (2.4.8)$$

and its trace is

$$T = -\rho_0 - 3\rho_0 \cos(2mt) = -\rho_0[1 + 3 \cos(2mt)] . \quad (2.4.9)$$

This gives the right-hand side of Eq. (2.4.2).

Finally, we can write down Eq. (2.4.2) as

$$-6\ddot{\Phi} + 2\nabla^2(2\Phi - \Psi) = \rho_0[1 + 3 \cos(2mt)] . \quad (2.4.10)$$

We are now in a position to determine the oscillating part of the gravitational potential. Let us separate the gravitational potential  $\Phi(\Psi)$  into the time-independent part  $\Phi_0(\Psi_0)$  and the time-dependent part  $\delta\Phi(\delta\Psi)$ . The time-independent part of the time-time component of Einstein's equation is Poisson's equation

$$2\nabla^2\Phi_0 = \rho_0 . \quad (2.4.11)$$

We also have the equation  $\Phi_0 = \Psi_0$  from the traceless part of the space-space component of Einstein's equation. Using above equations, Eq. (2.4.10) leads

$$-6\delta\ddot{\Phi} = 3\rho_0 \cos(2mt) , \quad (2.4.12)$$

where we assumed  $\delta\ddot{\Phi} \gg \nabla^2\delta\Phi$ . Integrating Eq. (2.4.12) twice, we obtain the oscillating part of the gravitational potential as

$$\delta\Phi = \frac{\rho_0}{8m^2} \cos(2mt) . \quad (2.4.13)$$

Note that the oscillating part  $\delta\Phi$  is much smaller than the constant part  $\Phi_0$  since  $k^2 \ll m^2$ . The amplitude  $|\delta\Phi|$  and the frequency  $f$  of the oscillating gravitational potential  $\delta\Phi$  are

$$|\delta\Phi| = \frac{\rho_0}{8m^2} = 4.8 \times 10^{-18} \left( \frac{\rho_0}{0.3 \text{ GeV/cm}^3} \right) \left( \frac{10^{-22} \text{ eV}}{m} \right)^2 , \quad (2.4.14)$$

$$f = \frac{2m}{2\pi} = 5 \times 10^{-8} \text{ Hz} \left( \frac{m}{10^{-22} \text{ eV}} \right) . \quad (2.4.15)$$

In the following subsections we see how to measure this oscillating gravitational potential.

## 2.4.2 Detection Method I: Pulsar Timing Array Experiments

In this subsection we discuss a detection method for the oscillating gravitational potential derived above using pulsar timing observations based on Sec. 3 of Ref. 2.

A pulsar is a rotating neutron star that emits a beam of electromagnetic radiation. We can see the beam only when the beam is pointing towards us. Thus we observe pulse signals from pulsars, which can be used as accurate clocks. The observable quantity by pulsar timing experiments is the timing residual, which is defined as

$$\Delta t(t) = - \int_0^t dt' \frac{\Omega(t') - \Omega_0}{\Omega_0} , \quad (2.4.16)$$

where  $\Omega_0$  is an emitted frequency at a pulsar,  $\Omega(t)$  is an observed frequency at an antenna. When the metric is constant in time, the emitted frequency remains to be unchanged and there is no change in the arrival time of the pulse signal. Assuming that a pulse with a frequency  $\Omega_0$  is emitted at  $(t', \mathbf{x}_p)$  and reaches us at  $(t, \mathbf{x})$ , the change in the frequency (redshift) can be written as

$$\frac{\Omega(t) - \Omega_0}{\Omega_0} = \Phi(t, \mathbf{x}) - \Phi(t', \mathbf{x}_p) - \int_{t'}^t dt'' n_i \partial_i [\Phi(t'', \mathbf{x}''(t'')) + \Psi(t'', \mathbf{x}''(t''))] , \quad (2.4.17)$$

where  $n_i$  is the direction of the propagation of the pulse signal. The path  $\mathbf{x}''(t'')$  is the trajectory on which the pulse signal propagates, i.e., the geodesic of the metric, and can be approximated as the straight line at the first order of the metric. Thus the time interval between the emission and detection is equivalent to the distance to the pulsar  $D (= t - t')$ . Since the distances to pulsars used in pulsar timing experiments are  $D \gtrsim 100 \text{ pc}$ , which is much larger than  $m^{-1} \sim 1 \text{ pc}$  for  $m = 10^{-22} \text{ eV}$ , the integrand in Eq. (2.4.17) is a rapidly oscillating function in the interval of integration. In addition, the size of the change in the metric (gravitational potential) is about  $|\nabla\Phi/\Phi| \sim |\nabla\Psi/\Psi| \sim k^{-1}$ , and we have a hierarchy  $k/m \sim v \sim 10^{-3}$ . Thus the integral in Eq. (2.4.17) is negligibly smaller than the

first two terms. Hence only  $\Phi$  affects the arrival time of pulse signals from pulsars. Since the time-independent part  $\Phi_0$  causes the constant shift of the frequency, which cannot be measured by pulsar timing experiments, the shift of the frequency can be written as

$$\frac{\Omega(t) - \Omega_0}{\Omega_0} = |\delta\Phi| [\cos(\omega t + 2\alpha(\mathbf{x})) - \cos(\omega(t - D) + 2\alpha(\mathbf{x}_p))] , \quad (2.4.18)$$

where  $|\delta\Phi| = \rho_0/8m^2$ . Here we explicitly write the phase of the oscillation  $\alpha$  since it can be important for pulsar timing observations. This is because a typical distance to pulsars is as large as or larger than the Jeans length. Substituting this into Eq. (2.4.16), we obtain the timing residual at time  $t$  as

$$\Delta t(t) = \frac{2|\delta\Phi|}{\omega} \sin(mD + \alpha(\mathbf{x}) - \alpha(\mathbf{x}_p)) \cos(\omega t + \alpha(\mathbf{x}) + \alpha(\mathbf{x}_p) - 2D/\omega) , \quad (2.4.19)$$

where we subtracted the averaged value, which does not affect the pulsar timing signal. The timing residual oscillates in time with an angular frequency  $\omega = 2m$ , and its amplitude is

$$|\Delta t| = \frac{2|\delta\Phi|}{\omega} \sin(2D/\omega + \alpha(\mathbf{x}) - \alpha(\mathbf{x}_p)) = \frac{\rho_0}{8m^2} \sin(mD + \alpha(\mathbf{x}) - \alpha(\mathbf{x}_p)) . \quad (2.4.20)$$

Currently we have no pulsar that has enough accuracy to detect the signal (2.4.19). However we can use a statistical method by using multiple pulsars. This is done by pulsar timing array experiments. Since pulsars are assumed to distribute randomly in the galaxy, the average value of  $\langle \Delta t \rangle$  over distances  $D$  and phases  $\alpha(\mathbf{x}_p)$  is zero. A nontrivial quantity is its variance, or equivalently, the root-mean-square value

$$\sqrt{\langle \Delta t^2 \rangle} = \frac{\sqrt{2}|\delta\Phi|}{\omega} . \quad (2.4.21)$$

Let us compare the stochastic signal of ultralight scalar field dark matter (2.4.21) to that of the stochastic gravitational waves, which is a target of the pulsar timing array experiments. The timing residual caused by a gravitational wave with an amplitude  $h$  and an angular frequency  $\omega$  is

$$\Delta t_{\text{GW}} = \frac{h}{\omega} \sin\left(\frac{\omega D(1 - \cos\theta)}{2}\right) (1 + \cos\theta) \sin(2\psi) , \quad (2.4.22)$$

where  $\theta$  is the angle between the source and the pulsar,  $\psi$  denotes the direction of the polarization of the gravitational wave. The root mean square of Eq. (2.4.22) over the distances  $D$  and the angles  $(\theta, \psi)$  gives

$$\sqrt{\langle \Delta t_{\text{GW}}^2 \rangle} = \frac{h_c}{\sqrt{3}\omega} , \quad (2.4.23)$$

where we replaced  $h$  with  $h_c$ , which is called the characteristic strain of the stochastic gravitational wave.

Comparing Eq. (2.4.21) with Eq. (2.4.23), the signal of ultralight scalar field dark matter on pulsar timing array experiments is equivalent to that of stochastic gravitational wave with an amplitude (characteristic strain)

$$h_c = 2\sqrt{3}|\delta\Phi| = 1.6 \times 10^{-15} \left( \frac{\rho_0}{0.3 \text{ GeV/cm}^3} \right) \left( \frac{10^{-23} \text{ eV}}{m} \right)^2. \quad (2.4.24)$$

A frequency of the signal is

$$f = \frac{\omega}{2\pi} = \frac{2m}{2\pi} = 5 \times 10^{-9} \text{ Hz} \left( \frac{m}{10^{-23} \text{ eV}} \right). \quad (2.4.25)$$

Here we normalized the mass of the scalar field by  $m = 10^{-23} \text{ eV}$  since pulsar timing array experiments have sensitivity at  $f \sim (\text{year})^{-1} \sim \text{nHz} \sim 10^{-23} \text{ eV}$ . The factor  $2\sqrt{3}$  in Eq. (2.4.24) comes from the geometrical difference between scalar and tensor (gravitational) waves, and two polarizations of gravitational waves.

In Fig. 2.3, the signal (2.4.24) is plotted as a function of the mass  $m$  with the sensitivity curves of current (PPTA) and planned (SKA) pulsar timing array experiments. Importantly, the future SKA experiment have enough sensitivity to detect the signal of ultralight scalar field dark matter.

We note that the amplitude of the signal is proportional to the local dark matter density, as shown in Eq. (2.4.14). Hence the future SKA experiment has a chance to detect the signal even when ultralight scalar field dark matter is sub-dominant component of dark matter. From Fig. (2.3), we expect that the SKA experiment have sensitivity down to a few percent fraction of ultralight scalar field dark matter.

### 2.4.3 Detection Method II: Laser Interferometers

In this subsection we introduce another method for detecting the oscillating gravitational potential using gravitational-wave interferometers. This subsection is based on Ref. 18.

The era of gravitational wave astronomy started on 14th September 2015, when the two interferometer detectors of the LIGO simultaneously observed a gravitational wave signal [20]. Now, we can measure tiny fluctuations of the spacetime by using these high precision laser interferometers. Since the solar system moves through the dark matter halo at the velocity of about  $v \sim 300 \text{ km/s} = 10^{-3}$ , the oscillating ultralight scalar field looks like scalar gravitational waves for us. Thus we can utilize the laser interferometers for detecting ultralight scalar field dark matter.

In the previous subsections we studied the oscillation of the gravitational potential in the halo reference frame. However, since an interferometer detector is moving through the dark matter halo, we need to solve Einstein's equation in the detector reference frame. The energy-momentum tensor of ultralight scalar field dark matter in the detector frame is given by the Lorentz-boost transformation

$$t' = \gamma(t + \mathbf{v} \cdot \mathbf{x}), \quad (2.4.26)$$

$$\mathbf{x}' = x^i + \frac{\gamma - 1}{v^2}(\mathbf{x} \cdot \mathbf{v})\mathbf{v} + \gamma\mathbf{v}t, \quad (2.4.27)$$

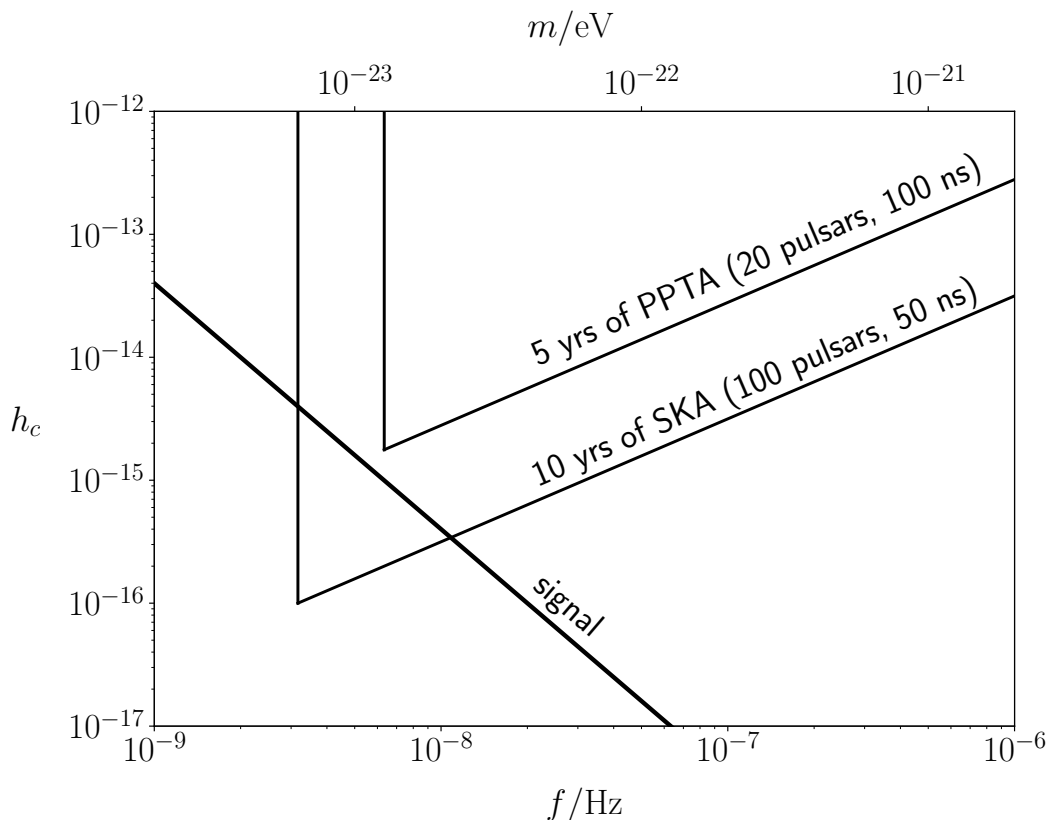


Figure 2.3: The signal (2.4.24) as a function of the frequency  $f = \omega/2\pi$  (lower axis) or the mass  $m$  (upper axis) with the sensitivity curves of the current (PPTA) and planned (SKA) pulsar timing array experiments. This figure is reproduced from Fig. 1 of Ref. 2.

where  $\mathbf{x}$  and  $\mathbf{x}'$  are the coordinate system attached to the halo and detector, respectively,  $\mathbf{v}$  is the relative velocity of the detector to the halo, and  $\gamma \equiv 1/\sqrt{1-v^2}$  is the Lorentz factor. Hence, the energy-momentum tensor in the detector frame is written as

$$T_{00} = \rho_0 \gamma^2 [1 - v^2 \cos(\omega t')] , \quad (2.4.28)$$

$$T_{0i} = \rho_0 \gamma^2 v_i [1 - \cos(\omega t')] , \quad (2.4.29)$$

$$T_{ij} = -\rho_0 \cos(\omega t') \delta_{ij} + \rho_0 \gamma^2 v_i v_j [1 - \cos(\omega t')] , \quad (2.4.30)$$

where  $t' = \gamma(t + \mathbf{v} \cdot \mathbf{x})$ .

As discussed before, we can neglect the expansion of the universe on the halo scale, and can treat the gravitational potentials can still be treated as perturbations. We use the Newtonian gauge for the metric:

$$g_{\mu\nu} = \begin{pmatrix} -1 - 2\Psi & 0 \\ 0 & (1 - 2\Phi)\delta_{ij} \end{pmatrix} + \delta\tilde{g}_{\mu\nu} , \quad (2.4.31)$$

where  $\delta\tilde{g}_{\mu\nu}$  is a constant tensor introduced for the consistency of Einstein's equation, which is produced by the constant velocity  $\mathbf{v}$ . We can calculate the Einstein tensor at the linear

order as

$$G_{00} = 2\nabla^2\Phi , \quad (2.4.32)$$

$$G_{0i} = 2\dot{\Phi}_{,i} + \tilde{G}_i , \quad (2.4.33)$$

$$G_{ij} = [2\ddot{\Phi} - \nabla^2(\Phi - \Psi)]\delta_{ij} + \partial_i\partial_j(\Phi - \Psi) + \tilde{G}_{ij} , \quad (2.4.34)$$

where  $\tilde{G}_i$  and  $\tilde{G}_{ij}$  are constant parts calculated from  $\delta\tilde{g}_{\mu\nu}$ .

Let us separate the gravitational potential  $\Phi$  ( $\Psi$ ) into the time-independent part  $\Phi_0$  ( $\Psi_0$ ) and the time-dependent part  $\delta\Phi$  ( $\delta\Psi$ ). As we will see later,  $\delta\Psi$  is the only observable quantity by interferometers. The time-independent part of the  $(0, 0)$  component of Einstein's equation is Poisson's equation:

$$2\nabla^2\Phi_0 = \rho\gamma^2 , \quad (2.4.35)$$

where  $\gamma^2 = 1 + \mathcal{O}(v^2)$ . The time-dependent part of the  $(0, 0)$  component of Einstein's equation gives

$$\delta\Phi(t, \vec{x}) = \frac{\rho}{8m^2} \cos[\omega\gamma(t + \vec{v} \cdot \vec{x})] . \quad (2.4.36)$$

Finally, we obtain  $\delta\Psi$  from the time-dependent part of the  $(i, j)$  component of Einstein's equation:

$$\delta\Psi(t, \vec{x}) = -\frac{\rho}{8m^2} \cos[\omega\gamma(t + \vec{v} \cdot \vec{x})] . \quad (2.4.37)$$

We can check that the other components of Einstein's equation are also satisfied.

Next we calculate the detector signal induced by the oscillating pressure of ultralight scalar field dark matter. We calculate the metric in the synchronous(-like) gauge by using a gauge transformation in order to know spatial fluctuations of the metric. The detector signal is then obtained by contracting the metric with a detector tensor.

The mechanism of an interferometer is simple. A laser light is sent on a beam-splitter which separates the light, with equal probability amplitudes, into a beam traveling in one arm and a beam traveling in a second orthogonal arm. At the end of each arm, there are totally reflecting mirrors. After traveling back and forth, the two beams recombine at the beam-splitter, and a part of the resulting beam goes to a photo-detector. Therefore, any variation in the length of the arms results in a corresponding variation of the power at the photo-detector. Indeed, using this interferometer, we can detect gravitational waves. Here, the idea is to utilize the interferometer detector for detecting ultralight scalar field dark matter.

An interferometer detector is characterized by the detector tensor

$$D_{ij} \equiv \frac{1}{2}(\hat{m}_i\hat{m}_j - \hat{n}_i\hat{n}_j) , \quad (2.4.38)$$

where  $\hat{m}$  and  $\hat{n}$  are the directions of the detector arms. The detector signal produced by spatial fluctuations of the metric  $h_{ij}$  is given by

$$s = D_{ij}h_{ij} . \quad (2.4.39)$$

In order to use this formula, we should transform all of the time-dependent part of the metric to the space-space component  $h_{ij}$ . Namely, we want to rewrite the time-dependent part of the metric as follows:

$$\delta g_{\mu\nu} = \begin{pmatrix} 0 & 0 \\ 0 & -2\delta A\delta_{ij} + 2\delta B_{,ij} \end{pmatrix}. \quad (2.4.40)$$

Note that we focus only on the time-dependent components, and thus this is not exactly the synchronous gauge. The signal in this gauge is given by

$$s = (\hat{m}_i\hat{m}_j - \hat{n}_i\hat{n}_j)\delta B_{,ij}. \quad (2.4.41)$$

Since  $D_{ij}\delta_{ij} = 0$  for any detector tensors,  $\delta A$  cannot be detected by interferometers. The gauge transformation gives  $\delta A = \delta\Phi$  and

$$\delta\ddot{B} = -\delta\Psi = \frac{\rho}{8m^2} \cos[\omega\gamma(t + \vec{v} \cdot \vec{x})]. \quad (2.4.42)$$

Hence, we obtain

$$\delta B_{,ij} = \frac{\rho}{8m^2} v_i v_j \cos[\omega\gamma(t + \vec{v} \cdot \vec{x})]. \quad (2.4.43)$$

We note that  $\delta B$  has ambiguity of a function  $f(\vec{x})t + g(\vec{x})$ . However, a constant function  $g(\vec{x})$  does not affect the signal and stationarity of the system requires that  $f(\vec{x})$  vanishes. Therefore, the signal from the oscillating pressure of the ultralight scalar field dark matter is given by

$$s(t) = \alpha \cdot \frac{\rho v^2}{8m^2} \cos(\omega\gamma t), \quad (2.4.44)$$

where  $\alpha \equiv |(\hat{v} \cdot \hat{m})^2 - (\hat{v} \cdot \hat{n})^2|$  is a geometric factor of  $\mathcal{O}(1)$ . We omitted the unimportant phase  $\omega\gamma\mathbf{v} \cdot \mathbf{x}_d$  of the signal, where  $\mathbf{x}_d$  is the position of the detector. The factor  $\alpha$  reaches the maximum when  $\mathbf{v}$  is parallel to  $\hat{m}$  or  $\hat{n}$ . If the angle between two arms is  $\theta$ , the maximum value of  $\alpha$  is  $\alpha_{\max} = 1 - \cos^2\theta$ . A typical amplitude of the signal is <sup>2</sup>

$$\frac{\rho v^2}{8m^2} = 4.8 \times 10^{-24} \left(\frac{v}{10^{-3}}\right)^2 \left(\frac{10^{-22} \text{ eV}}{m}\right)^2, \quad (2.4.45)$$

where we assumed  $\rho = 0.3 \text{ GeV/cm}^3$ . The corresponding frequency is

$$f = \frac{\omega\gamma}{2\pi} \simeq 5 \times 10^{-8} \text{ Hz} \left(\frac{m}{10^{-22} \text{ eV}}\right). \quad (2.4.46)$$

Apparently, the signal is proportional to  $m^{-2}$  and  $v^2$ . Hence, the lower the mass is, the easier we can detect the ultralight scalar field dark matter wind.

A typical detector signal (2.4.44) with  $\alpha = 1$  and sensitivity curves of planned laser interferometer experiments (DECIGO, LISA, and ASTROD-GW) are plotted in Fig. 2.4. If we were able to construct a space-based interferometer with strain sensitivity  $10^{-24}$ ,

<sup>2</sup> In evaluating Eq. (23) in Ref. 18, we missed a factor 0.3 of  $\rho_0 = 0.3 \text{ GeV/cm}^3$ . Thus the value in Eq. (2.4.45) is smaller than that of Eq. (23) in Ref. 18 by a factor of 0.3.

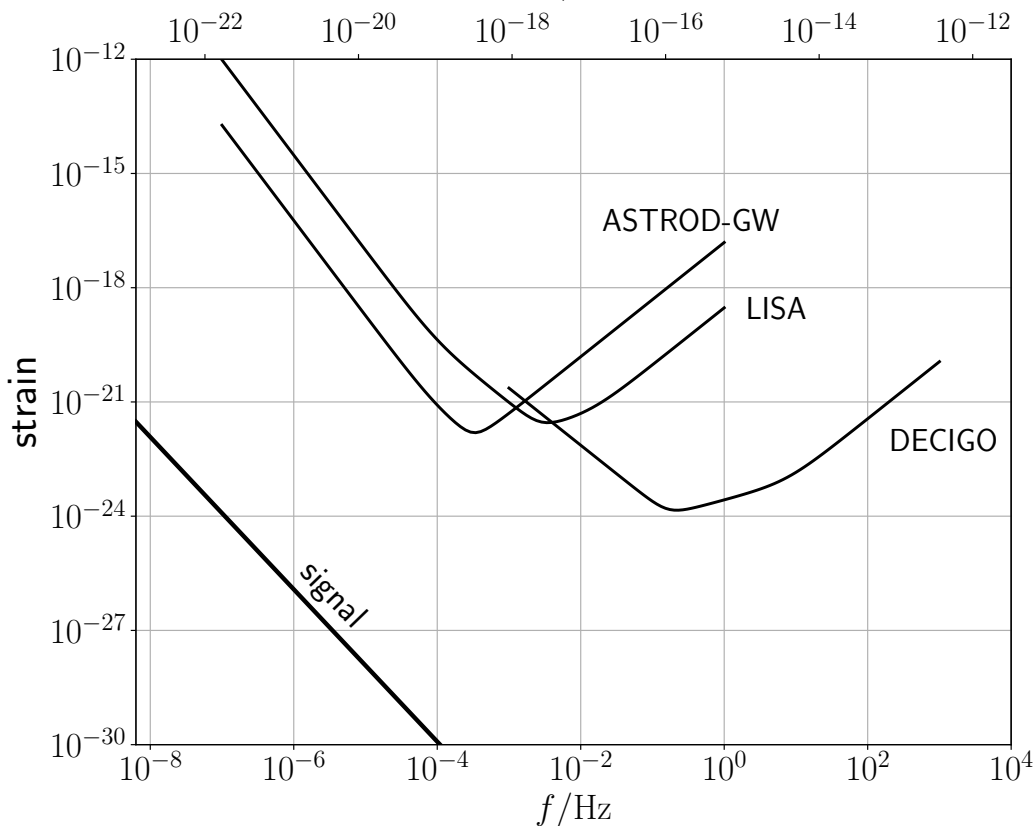


Figure 2.4: A typical detector signal (2.4.44) with  $\alpha = 1$  and sensitivity curves of planned laser interferometer experiments, DECIGO, LISA, and ASTROD-GW [21]. This figure is reproduced from Fig. 1 of Ref. 18.

which is similar as that of the DECIGO, in the appropriate frequency band, we would be able to observe the ultralight scalar field dark matter wind up to  $1.8 \times 10^{-22}$  eV. Though constructing an interferometer with enough sensitivity for detecting the signal is beyond current technical capabilities, we believe that it will be realized by future technological innovations.

We should mention that the velocity  $\mathbf{v}$ , which we have treated as a constant in the analysis, actually varies in time. Since the earth moves around the sun with a velocity about  $30 \text{ km/s} = 10^{-4}$ ,  $v = |\mathbf{v}|$  varies by about 10% in one year. However, we believe that such an annual modulation in the signal can be extracted as a noise.

# Chapter 3

## Modified Gravity Theories

In this chapter modified gravity theories are reviewed. In Sec. 3.1, motivations for considering alternative theories of gravity are explained. In Sec. 3.2, we review the  $f(R)$  theory as an example of modified gravity theories. The constraints on the  $f(R)$  models are discussed in Sec. 3.3.

### 3.1 Motivations for Alternative Theories of Gravity

The theory of general relativity is widely thought to be a fundamental theory of gravity that describes the geometric properties of spacetime. In fact, a large number of observations prove the success of general relativity. However, there are some reasons to assume that the theory of gravity should be different from Einstein's theory.

A major reason to consider alternative theory of gravity is the existence of two eras of accelerated expansion of the universe. The earlier one is cosmic inflation, which is thought to be necessary to explain why the present universe is so homogeneous and isotropic (the horizon problem), and flat (the flatness problem). The inflationary expansion is assumed to have took place just after the birth of the universe, which is accompanied by the standard big bang cosmology. One small patch of the universe expands exponentially, and the observable universe today is regarded as a part of the homogeneous and flat patch. In this way, inflation can resolve the problems in the big bang cosmology naturally. The existence of the epoch of inflation also predicts the primordial fluctuations of matter density, which is considered to be a seed of galaxies and the CMB. In fact, the value of a parameter known as the spectral index, which characterizes the initial matter power spectrum, is consistent with prediction of inflation. Although the cosmological constant can cause inflationary expansion of the universe, it is not responsible for inflation since the inflationary epoch must end to connect to the big bang universe. One way to have an inflationary phase is to introduce a scalar field (inflaton) that rolls down slowly on its potential. The potential energy of the inflaton causes quasi-de Sitter expansion of the universe. Another way is to modify Einstein's theory of gravity. Currently, the so-called Starobinsky-type  $f(R)$  model of inflation [22] is most favored by the CMB observations.

We also know that the present universe is in another accelerating phase. An unknown

component that should be introduced to explain this late time acceleration is called dark energy. Unlike inflation, dark energy can be explained by the cosmological constant. However, we have some unnaturalness problems on the cosmological constant as mentioned in Sec. 1.1. One way to realize the late time acceleration is introducing a scalar field called quintessence. The mechanism is qualitatively the same as in the case of inflation, while the energy scale is much lower than that of inflation. Of course, we can assume the theory of gravity is different from Einstein's general relativity on cosmological scale. In the moment, there is no evidence which one of a scalar field (inflaton or quintessence) and modified gravity theories is favored. Hence it is important to investigate both possibilities in detail.

## 3.2 $f(R)$ Theory

In this thesis we focus on the  $f(R)$  theory among a number of modified gravity theories. This is because the  $f(R)$  theory is one of the simplest modified gravity theories, and at the same time it contains rich phenomena as seen in Chap. 4 and Chap. 5.

In Subsec. 3.2.1 we review the  $f(R)$  theory. We summarize the equations to be used in this thesis there, We also explain how (quasi-)de Sitter expansion is realized in this theory. In Subsec. 3.2.2 we move onto the so-called scalar-tensor formalism of the  $f(R)$  theory, which is useful for understanding the physics and also for numerical calculations. We discuss the relation between the  $f(R)$  theory and other modified gravity theories in Subsec. 3.2.3.

Many topics on the  $f(R)$  theory are covered in Ref. 23 by De Felice and Tsujikawa. For details see this review paper and the references therein.

### 3.2.1 Overview of $f(R)$ Theory

The  $f(R)$  theory is defined by the action

$$S_G = \frac{1}{2} \int d^4x \sqrt{-g} [R + f(R)] , \quad (3.2.1)$$

where  $f(R)$  is an arbitrary function of the Ricci scalar  $R$ . Equivalently, the action (3.2.1) is sometimes written as

$$S_G = \frac{1}{2} \int d^4x \sqrt{-g} F(R) , \quad (3.2.2)$$

where  $F(R) \equiv R + f(R)$ . In this theory, matter fields are assumed to minimally couple to the metric. With writing the action of matter fields as  $S_M$ , the total action of the system

is  $S = S_G + S_M$ . The variation of the total action  $S$  with respect to the metric gives<sup>1</sup>

$$G_{\mu\nu} - \frac{1}{2}g_{\mu\nu}f(R) + [R_{\mu\nu} + g_{\mu\nu}\square - \nabla_\mu\nabla_\nu]f_R = T_{\mu\nu} , \quad (3.2.3)$$

where  $T_{\mu\nu}$  is the energy-momentum tensor of matter fields. Note that Eq. (3.2.3) reduces to Einstein's equation in the general relativity (with the cosmological constant), where  $f(R) = -2\Lambda$  and  $f_R = 0$ . The trace of Eq. (3.2.3) gives

$$-R - 2f(R) + (R + 3\square)f_R = T , \quad (3.2.4)$$

where  $T \equiv g^{\mu\nu}T_{\mu\nu}$  is the trace of the energy-momentum tensor. This is understood as the equation of motion for  $f_R$ . Thus this shows that there is a new degree of freedom  $f_R$  that propagates in the 4-dimensional spacetime in addition to two degrees of freedom of the standard gravitational waves. In the next subsection, we see this new degree of freedom explicitly by moving onto the scalar-tensor formalism of the  $f(R)$  theory.

Next we discuss how (quasi-)de Sitter expansion is realized. Let us find the de Sitter point in the vacuum ( $T = 0$ ), at which the Ricci scalar is a positive constant. The equation to determine the de Sitter point is given by setting  $\square f_R = 0$  and  $T = 0$  in Eq. (3.2.4) as

$$-R - 2f(R) + Rf_R = 0 , \quad (3.2.5)$$

Equivalently, we can write Eq. (3.2.5) as

$$RF_R - 2F(R) = 0 , \quad (3.2.6)$$

where  $F_R \equiv dF(R)/dR$ . If we see Eq. (3.2.6) as a differential equation for  $F(R)$  with respect to  $R$ , the solution is  $F(R) = \alpha R^2$ . Hence the model  $F(R) = \alpha R^2$  has an exact de Sitter solution. For general models, however, the de Sitter condition, Eq. (3.2.5) or Eq. (3.2.6), is only satisfied for some particular value of  $R$ . This de Sitter point can be used for both inflation and dark energy.

### 3.2.2 Scalar-Tensor Formalism of $f(R)$ Theory

In the previous subsection, we have written down the field equation in the  $f(R)$  theory and seen that there is a new propagating degree of freedom  $f_R$  in the theory. In order to see this more clearly, we move onto the so-called scalar-tensor formalism of the  $f(R)$  theory by using change of variables.

---

<sup>1</sup> There are two different formalisms in deriving field equations in the  $f(R)$  theory, which are known as the metric formalism and the Palatini formalism. In the metric formalism, we assume that the affine connection is derived from the metric, that is, the affine connection is nothing but the Christoffel symbol. In the so-called Palatini formalism, we regard the affine connection as an independent variable, which does not depend on the metric. These two formalisms generally give rise to the different field equations. We note that the two formalisms give the same field equation, Einstein's equation, in general relativity. In this thesis, we use the metric formalism in deriving the field equation in the  $f(R)$  theory.

It is useful to use Eq. (3.2.2) for the action. Introducing an auxiliary field  $A$ , the action can be rewritten as

$$S_G = \frac{1}{2} \int d^4x \sqrt{-g} [F'(A)(R - A) + F(A)] . \quad (3.2.7)$$

The variation with respect to  $A$  gives the constraint condition  $F''(A)(R - A) = 0$ . Thus as far as  $F''(A) = f''(A) \neq 0$ , we have  $A = R$ . Substituting this relation into the action (3.2.7), we obtain the original action (3.2.2). Hence, the two theories (3.2.2) and (3.2.7) are equivalent as far as  $F''(A) = f''(A) \neq 0$ . Hereafter we assume the function  $f(R)$  is chosen to satisfy  $f''(R) \neq 0$ .

Let us define a scalar field  $\varphi = f'(A)$ , which is often called the *scalon*. In order for this transformation to be regular (invertible), we need the condition  $f''(A) \neq 0$ , which is already satisfied by the assumption. The action can be written in terms of the scalar field  $\varphi$  as

$$S_G = \frac{1}{2} \int d^4x \sqrt{-g} [(1 + \varphi)R - 2U(\varphi)] , \quad (3.2.8)$$

where the function  $U(\varphi)$  is defined as

$$U(\varphi) \equiv \frac{1}{2} [\varphi A(\varphi) - f(A(\varphi))] . \quad (3.2.9)$$

The theory (3.2.8) is in a category of the scalar-tensor theory, where a scalar field  $\varphi$  couples to the Ricci scalar as  $\varphi R$ . Hence, we have shown that  $f(R)$  theory is equivalent to a special case of the scalar-tensor theory.

The variation of the action (3.2.8) with respect to the scalaron field  $\varphi$  gives

$$R = 2U_{,\varphi} , \quad (3.2.10)$$

where  $U_{,\varphi} \equiv dU(\varphi)/d\varphi$ . Hence the Ricci scalar  $R$  is determined by the scalar field  $\varphi$ . This is in contrast to the case of the general relativity, where the Ricci scalar is fixed by the matter fields,  $R = -T$ .

On the other hand, the variation of the action (3.2.8) with respect to the metric gives the field equation

$$(1 + \varphi)G_{\mu\nu} + g_{\mu\nu}U(\varphi) + (g_{\mu\nu}\square - \nabla_\mu \nabla_\nu) = T_{\mu\nu} . \quad (3.2.11)$$

This is of course equivalent to Eq. (3.2.3). Trace of Eq. (3.2.11) gives the equation of motion for the scalaron field

$$3\square\varphi - (1 + \varphi)R + 4U(\varphi) = T . \quad (3.2.12)$$

Using Eq. (3.2.10), the equation of motion can be rewritten as

$$\square\varphi - V_{,\varphi} = \frac{T}{3} , \quad (3.2.13)$$

where we defined the potential  $V(\varphi)$  by

$$V_{,\varphi} \equiv \frac{1}{3} [2U_{,\varphi}(1 + \varphi) - 4U(\varphi)] . \quad (3.2.14)$$

The equation of motion (3.2.13) shows the scalaron field does propagate in the vacuum  $T = 0$  in the same way as the gravitational waves.

Assuming  $f(A) \ll A$  and  $\varphi = f'(A) \ll 1$  as usual, the gradient of the potential can be approximated as

$$V_{,\varphi} \simeq \frac{A(\varphi)}{3} . \quad (3.2.15)$$

We also have the following relation in this limit

$$R \simeq A(\varphi) . \quad (3.2.16)$$

We will use these approximated forms in analyzing specific models in Chap. 5.

### 3.2.3 Relation to Other Modified Gravity Theories

In this subsection we see some modified gravity theories other than the  $f(R)$  theory. The purpose here is to see that the analysis that will be done for the  $f(R)$  theory in the next two chapters can be easily generalized for other modified gravity theories.

The most famous alternative to Einstein's theory of general relativity would be the Brans-Dicke theory [24], which is in a category of the scalar-tensor theory. Here we introduce an extended form of the Brans-Dicke theory defined by

$$S_G = \frac{1}{2} \int d^4x \sqrt{-g} \left[ \phi R - \frac{\omega_{\text{BD}}}{\phi} (\partial\phi)^2 - 2U(\phi) \right] , \quad (3.2.17)$$

where  $\omega_{\text{BD}}$  is called the Brans-Dicke parameter and  $U(\phi)$  is a function of  $\phi$ . Note that the original Brans-Dicke theory has no potential term,  $U(\phi) = 0$ . In this theory the scalaron field  $\phi$  plays a roll of  $(8\pi G)^{-1}$ , that is, the gravitational constant is changed as  $G_{\text{eff}} = (8\pi\phi)^{-1}$ . Clearly, by identifying  $\phi = 1 + \varphi$ , the  $f(R)$  theory is a special case of the extended Brans-Dicke theory with  $\omega_{\text{BD}} = 0$ . Note that the  $f(R)$  theory in the Palatini formalism is equivalent to the case  $\omega_{\text{BD}} = -3/2$ . We can derive the equation of motion for the scalaron field  $\phi$  as

$$(3 + 2\omega_{\text{BD}})\square\phi + 4U(\phi) - 2\phi U_{,\phi} = T . \quad (3.2.18)$$

This reduces to Eq. (3.2.13) when  $\omega_{\text{BD}} = 0$ . The relation between the Ricci scalar and the scalaron field is

$$R = 2U_{,\phi} - \frac{\omega_{\text{BD}}}{\phi^2} [(\partial\phi)^2 + 2\phi\square\phi] , \quad (3.2.19)$$

which again reduces to the case of  $f(R)$  theory, Eq. (3.2.10), when  $\omega_{\text{BD}} = 0$ . Hence, in the Brans-Dicke theory, the scalaron field is sourced by the trace of the energy-momentum tensor, and then the Ricci scalar is determined by the scalaron field. This is qualitatively the same situation as in the  $f(R)$  theory.

Further extensions can be done by, for example, generalizing  $\omega_{\text{BD}}$  to be a function of  $\phi$  or adding the higher derivative interactions like  $(\square\phi)^2$ . An example is the Horndeski theory [25], which is the most general theory of gravity that leads to the second order

equations of motion. Even for such generalized theories, the situation that the scalaron field is sourced by matter fields and the Ricci scalar is determined by the scalaron field is qualitatively the same as in the  $f(R)$  theory. Moreover, it is known that a wide class of modified gravity theories can be reduced to the scalar-tensor theory at least in some limiting case. Hence the analysis that will be done for the  $f(R)$  theory is expected to be generalized to more general theories of modified gravity.

### 3.3 Constraints on $f(R)$ Theory

In this section we discuss constraints on  $f(R)$  models. In Subsec. 3.3.1 we derive the so-called local gravity constraints of  $f(R)$  models. These constraints are mainly from observations in the solar system, and all the models should pass these constraints. In Subsec. 3.3.2 we discuss the condition for  $f(R)$  models to explain dark energy. If we would like  $f(R)$  models to behave as dark energy, we have to impose this condition on the models. We make some comments on the constraints from the speed of gravitational wave in Subsec. 3.3.3.

#### 3.3.1 Local Gravity Constraints

For a constant energy density  $\rho$  and negligible pressure, we can define the effective potential of the scalaron field  $V_{\text{eff}}(\varphi)$  as

$$V_{\text{eff},\varphi} \equiv V_{,\varphi} - \frac{\rho}{3} . \quad (3.3.1)$$

Using the approximation  $V_{,\varphi} \simeq A(\varphi)/3$ , the gradient of the effective potential can be approximated as

$$V_{\text{eff},\varphi} \simeq \frac{1}{3}[A(\varphi) - \rho] . \quad (3.3.2)$$

Hence the minimum of the effective potential is determined by the condition  $A(\varphi) \simeq \rho$ . The mass of the scalaron field  $M$  is given by

$$M^2 \equiv V_{\text{eff},\varphi\varphi}(\varphi_0) = V_{,\varphi\varphi}(\varphi_0) , \quad (3.3.3)$$

where  $\varphi_0$  is the value at the minimum of  $V_{\text{eff}}(\varphi)$ . Since  $\varphi_0$  is determined by  $\rho$ , the mass of the scalaron depends on the surrounding energy density  $\rho$  in the  $f(R)$  theory. As we will see explicitly in Chap. 5, the mass becomes larger as the energy density  $\rho$  increases. This phenomenon is called the chameleon mechanism [26, 27].

Let us consider a spherically symmetric body with radius  $R_\alpha$  and mass  $M_\alpha$ . We suppose the energy density inside the body is a constant  $\rho_\alpha (= 3M_\alpha/4\pi R_\alpha^3)$  for simplicity. We denote the density outside the body as  $\rho_0 (\ll \rho_\alpha)$ . The values of the scalaron field at the minimum of the effective potential for  $\rho_\alpha$  and  $\rho_0$  are denoted as  $\varphi_\alpha$  and  $\varphi_0$ , respectively. Usually the condition  $\rho_\alpha \gg \rho_0$  leads  $|\varphi_\alpha| \ll |\varphi_0|$ . By analyzing the configuration inside and outside the

body, we obtain the gravitational potentials outside the body as

$$\Psi(r) = -\frac{GM_\alpha}{r} \left[ 1 + \epsilon_{\text{th},\alpha} \left( 1 - \frac{r}{R_\alpha} \right) \right] , \quad (3.3.4)$$

$$\Phi(r) = -\frac{GM_\alpha}{r} (1 - \epsilon_{\text{th},\alpha}) , \quad (3.3.5)$$

where we defined the so-called thin-shell parameter  $\epsilon_{\text{th},\alpha}$  as

$$\epsilon_{\text{th},\alpha} \equiv -\frac{\varphi_0 - \varphi_\alpha}{2GM_\alpha/R_\alpha} . \quad (3.3.6)$$

Assuming the hierarchy  $|\varphi_\alpha| \ll |\varphi_0|$  and denoting the gravitational potential at the surface of the body as  $\Phi_\alpha \equiv -GM_\alpha/R_\alpha$ , we obtain

$$\epsilon_{\text{th},\alpha} \simeq \frac{\varphi_0}{2\Phi_\alpha} . \quad (3.3.7)$$

Since  $\epsilon_{\text{th},\alpha} = 0$  in general relativity, the thin-shell parameter characterizes the deviation from Einstein's theory.

**Constraint on post-Newtonian parameter** Let us focus on a parameter  $\gamma$  defined as

$$\gamma \equiv \frac{\Phi}{\Psi} , \quad (3.3.8)$$

which is one of the so-called post-Newtonian parameters. In general relativity we have  $\gamma = 1$ . The tightest experimental bound on  $\gamma$  is

$$|\gamma - 1| < 2.3 \times 10^{-5} , \quad (3.3.9)$$

which comes from the time-delay effect of the Cassini tracking for the sun [28]. From Eq. (3.3.4) and Eq. (3.3.5), we can calculate the parameter  $\gamma$  at the surface of the object  $r = R_\alpha$  as

$$\gamma = 1 - \epsilon_{\text{th},\alpha} . \quad (3.3.10)$$

Thus the constraint (3.3.9) gives

$$|\epsilon_{\text{th},\odot}| = \left| \frac{\varphi_0}{2\Phi_\odot} \right| < 2.3 \times 10^{-5} , \quad (3.3.11)$$

where  $\odot$  denotes the sun. Using the value  $|\Phi_\odot| \simeq 2.1 \times 10^{-6}$ , we obtain the constraint on the scalaron field as

$$|\varphi_0| < 9.7 \times 10^{-11} . \quad (3.3.12)$$

**Constraint from violation of equivalence principle** Let us discuss the constraint on the thin-shell parameters from the possible violation of the equivalence principle. The experimental bound on the difference between the free-fall acceleration of the earth ( $a_{\oplus}$ ) and the moon ( $a_{\text{moon}}$ ) toward the sun is [29]

$$\frac{|a_{\oplus} - a_{\text{moon}}|}{|a_{\oplus} + a_{\text{moon}}|/2} < 10^{-13} . \quad (3.3.13)$$

We can evaluate the accelerations  $a_{\oplus}$  and  $a_{\text{moon}}$  as

$$a_{\oplus} \simeq \frac{GM_{\odot}}{r^2} \left[ 1 + 3\epsilon_{\text{th},\oplus}^2 \cdot \frac{\Phi_{\oplus}}{\Phi_{\odot}} \right] , \quad (3.3.14)$$

$$a_{\text{moon}} \simeq \frac{GM_{\odot}}{r^2} \left[ 1 + 3\epsilon_{\text{th},\text{moon}}^2 \cdot \frac{\Phi_{\text{moon}}}{\Phi_{\odot}} \right] . \quad (3.3.15)$$

Since we can rewrite  $\epsilon_{\text{th},\text{moon}}$  as

$$\epsilon_{\text{th},\text{moon}} \simeq \frac{\varphi_0}{2\Phi_{\text{moon}}} = \frac{\varphi_0}{2\Phi_{\oplus}} \cdot \frac{\Phi_{\oplus}}{\Phi_{\text{moon}}} \simeq \epsilon_{\text{th},\oplus} \cdot \frac{\Phi_{\oplus}}{\Phi_{\text{moon}}} , \quad (3.3.16)$$

the acceleration of the moon  $a_{\text{moon}}$  can be rewritten as

$$a_{\text{moon}} \simeq \frac{GM_{\odot}}{r^2} \left[ 1 + 3\epsilon_{\text{th},\oplus}^2 \cdot \frac{\Phi_{\oplus}^2}{\Phi_{\odot}\Phi_{\text{moon}}} \right] . \quad (3.3.17)$$

Using the values  $|\Phi_{\odot}| \simeq 2.1 \times 10^{-6}$ ,  $|\Phi_{\oplus}| \simeq 7.0 \times 10^{-10}$ , and  $|\Phi_{\text{moon}}| \simeq 3.1 \times 10^{-11}$ , the constraint (3.3.13) gives

$$|\epsilon_{\text{th},\oplus}| < 2.2 \times 10^{-6} . \quad (3.3.18)$$

Since  $\epsilon_{\text{th},\oplus} \simeq |\varphi_0/2\Phi_{\oplus}|$ , this leads

$$|\varphi_0| < 3.0 \times 10^{-15} . \quad (3.3.19)$$

This is tighter than Eq. (3.3.12), and then we use Eq. (3.3.19) for the local gravity constraints.

### 3.3.2 Cosmological Constraints

In this subsection we focus on the possibility that the  $f(R)$  theory explain dark energy. The constraint on  $f(R)$  models obtained here is only applied to specific models (the Hu-Sawicki model and the Starobinsky model) discussed in Sec. 5.3. In order to obtain constraints from cosmological observations such as the CMB, we should perform cosmological perturbations. However we just focus on the background evolution of the universe here, and obtain one necessary condition for the model to have the stage of (quasi-)de Sitter expansion.

As we saw in Subsec. 3.2.1, the  $f(R)$  theory has the de Sitter point satisfying Eq. (3.2.6). For convenience, let us define the following quantities:

$$r \equiv -\frac{d \ln F}{d \ln R} = -\frac{RF_{,R}}{F} , \quad (3.3.20)$$

$$m \equiv \frac{d \ln F_{,R}}{d \ln R} = \frac{RF_{,RR}}{F_{,R}} , \quad (3.3.21)$$

where  $F(R) = R + f(R)$ . The de Sitter point corresponds to  $r = -2$ . For general relativity with the cosmological constant,  $F(R) = R - 2\Lambda$ , we have  $m = 0$  since  $F_{,RR} = 0$ . Hence the quantity  $m$  characterizes the deviation from general relativity. Since both  $r$  and  $m$  are functions of  $R$ , we can write  $m$  as a function of  $r$ , i.e.,  $m(r)$ . The background evolution of all the  $f(R)$  models are characterized by the function  $m(r)$ . By analyzing stability of the de Sitter point, we obtain the following condition [30]:

$$0 < m(r = -2) \leq 1 . \quad (3.3.22)$$

In this thesis we only impose this condition for cosmologically viable  $f(R)$  models, and we just call this condition “cosmological constraint.”

### 3.3.3 Constraints from Speed of Gravitational Wave

Before closing the section, we would like to mention the detections of gravitational waves. The observation of a gravitational wave (GW170817) accompanied by electromagnetic radiation has allowed to set very stringent constraints on the propagation speed of gravitational waves. The relative difference of the speed of gravitational waves and that of light is constrained to be less than one part in  $10^{15}$  [31]. Thus modified gravity theories that predict the change in the speed of gravitational waves are essentially excluded, otherwise we need unacceptable fine tunings. In the  $f(R)$  theory the propagation speed of gravitational waves remains unchanged relative to that in the general relativity. Hence there is essentially no constraint on the  $f(R)$  theory from the observations of gravitational waves.

# Chapter 4

## Ultralight Scalar Field Dark Matter in $f(R)$ Theory I: Formalism

In Sec. 2.4, we studied the phenomenon caused by the oscillating pressure of ultralight scalar field dark matter based on Einstein's theory of gravity. The purpose of this research is to investigate how the phenomenon changes in the framework of modified gravity theories.

In this chapter we derive the formula for calculating the oscillating gravitational potential in the framework of the  $f(R)$  theory. We first discuss the  $f(R)$  formulation in Sec. 4.1. Then we move onto the equivalent scalar-tensor formalism in Sec. 4.2. The scalar-tensor formalism is more useful to understand the phenomenon qualitatively and also for numerical calculations. This chapter is based on Ref. 19 and Ref. 32.

### 4.1 Formulation in $f(R)$ Theory

We start with the field equation for the metric in the  $f(R)$  theory (see Subsec. 3.2.1 for the derivation):

$$G_{\mu\nu} - \frac{1}{2}g_{\mu\nu}f + (R_{\mu\nu} + g_{\mu\nu}\square - \nabla_\mu\nabla_\nu)f_R = T_{\mu\nu} , \quad (4.1.1)$$

where  $f_R \equiv df(R)/dR$ . Note that this is the same as Eq. (3.2.3). The trace of the field equation gives

$$3\square f_R - R + Rf_R - 2f = T , \quad (4.1.2)$$

where  $T \equiv g^{\mu\nu}T_{\mu\nu}$ . This equation is understood as the equation of motion for  $f_R$ .

In the  $f(R)$  theory, we usually assume  $f(R) \ll R$  and  $f_R \ll 1$  on galactic or smaller scales in order not to spoil the success of Einstein's theory. Without these assumptions, we will have a wrong relation between the gravitational potentials and the matter energy density. Then we obtain the following equation

$$3\square f_R - R = T . \quad (4.1.3)$$

Hereafter we assume the energy-momentum tensor of matter field is dominated by ultralight scalar field dark matter. Since we assume the ultralight scalar field minimally couples

to gravity even in  $f(R)$  theory, we can use the same form for the energy-momentum tensor as that in Einstein's theory:

$$T_{\mu\nu} = \begin{pmatrix} \rho_0 & 0 \\ 0 & -\rho_0 \cos(2mt)\delta_{ij} \end{pmatrix}. \quad (4.1.4)$$

The new degree of freedom  $f_R$  is sourced by the trace of this energy-momentum tensor

$$T = g^{\mu\nu}T_{\mu\nu} \simeq \eta^{\mu\nu}T_{\mu\nu} = -\rho_0[1 + 3 \cos(2mt)], \quad (4.1.5)$$

where we ignored small quantities proportional to the metric perturbations.

Let us evaluate the term  $\square f_R$ . The time dependence of  $f_R$  is determined by the oscillating part of the source term. Thus we can evaluate the time-dependence of  $f_R$  as  $|\dot{f}_R| \sim (2m)^2|f_R|$  with  $m^{-1} \sim 0.1 \text{ pc}$  for  $m = 10^{-22} \text{ eV}$ . On the other hand, the spacial derivative of  $f_R$  is evaluated as  $|\nabla^2 f_R| \sim k^2|f_R|$  with  $k \gtrsim (10 \text{ kpc})^{-1}$ , which corresponds to a typical length scale of the dark matter halo. Since  $m^2 \gg k^2$ , we can assume  $\square f_R \simeq -\ddot{f}_R$ . We use this kind of approximation throughout this chapter. Under the assumption, the field equation can be approximated as

$$3\ddot{f}_R + R = -T. \quad (4.1.6)$$

We should note that the contribution of the first term in Eq. (4.1.6) is not so small compared to the second one though we assume  $f_R \ll 1$ . This is because the  $f_R$  term appears as  $\ddot{f}_R \sim (2m)^2 f_R$ , and is enhanced by a factor of  $m^2/R_0 = m^2/\rho_0 \sim 10^{17}(m/10^{-22} \text{ eV})^2$ . Thus the first term in Eq. (4.1.6) can be comparable to the second term, the Ricci scalar  $R$ .

As in Subsec. 2.4.1, we use the Newtonian gauge for the metric:

$$g_{\mu\nu} = \begin{pmatrix} -1 - 2\Psi & 0 \\ 0 & (1 - 2\Phi)\delta_{ij} \end{pmatrix}. \quad (4.1.7)$$

At the first order of the potentials, the Ricci scalar is calculated as

$$R = -6\ddot{\Phi} + 2\nabla^2(2\Phi - \Psi). \quad (4.1.8)$$

Let us write the Ricci scalar  $R$  as the sum of the time-independent part  $R_0$  and the time-dependent part  $\delta R$ :

$$R = R_0 + \delta R. \quad (4.1.9)$$

The time-independent part  $R_0$  is defined as the average value of  $R$  over time much longer than the period of the oscillation. Hereafter we write this kind of time average using the bracket symbol  $\langle \dots \rangle$ . Hence  $R_0 \equiv \langle R \rangle$ . We also separate the gravitational potential  $\Phi$  ( $\Psi$ ) into the time-independent part  $\Phi_0 \equiv \langle \Phi \rangle$  ( $\Psi_0 \equiv \langle \Psi \rangle$ ) and the time-dependent part  $\delta\Phi$  ( $\delta\Psi$ ). With this separation, the Ricci scalar can be approximated as

$$R \simeq -6\delta\ddot{\Phi} + 2\nabla^2(2\Phi_0 - \Psi_0), \quad (4.1.10)$$

where we assumed  $|\delta\ddot{\Phi}| \gg |\nabla^2\delta\Phi|$  and  $|\delta\ddot{\Phi}| \gg |\nabla^2\delta\Psi|$  as before. Since  $\langle\delta\ddot{\Phi}\rangle = 0$  as far as  $\delta\ddot{\Phi}$  is finite, we obtain  $R_0$  and  $\delta R$  as

$$R_0 = 2\nabla^2(2\Phi_0 - \Psi_0) , \quad (4.1.11)$$

$$\delta R = -6\delta\ddot{\Phi} . \quad (4.1.12)$$

The space-space component of Einstein's equation gives the relation  $\Phi_0 = \Psi_0$ . Thus  $R_0$  can be written as  $R_0 = 2\nabla^2\Phi_0$ . By time-averaging the field equation (4.1.6), we have  $R_0 = \langle -T \rangle = \rho_0$ . Hence we have the equation

$$2\nabla^2\Phi_0 = \rho_0 , \quad (4.1.13)$$

which is nothing but Poisson's equation. Integrating Eq. (4.1.12) with respect to time twice and using the field equation (4.1.6), we obtain

$$\delta\Phi = \frac{\rho_0}{8m^2} \cos(2mt) + \frac{1}{2}(f_R - \langle f_R \rangle) , \quad (4.1.14)$$

where  $\langle f_R \rangle$  is the average value of  $f_R$ . The first term in Eq. (4.1.14) is the same as in the Einstein's theory, Eq. (2.4.13). This is consistent with the fact that  $f_R = 0$  in Einstein's theory.

In summary, all we have to do for calculating the amplitude of the oscillating gravitational potential is solving the field equation (4.1.6) and then substituting the solution into Eq. (4.1.14). A peculiar feature of the  $f(R)$  theory can be seen when the second term in Eq. (4.1.14) becomes comparable to or larger than the first term.

## 4.2 Formulation in Scalar-Tensor Theory

In the previous section, we have derived the formula for calculating the oscillating part of the gravitational potential sourced by the oscillating pressure of ultralight scalar field dark matter. Though the form of Eq. (4.1.14) is simple, it is not so easy to understand the physics governed by the equation. In this section we move onto the scalar-tensor formalism of the  $f(R)$  theory, which is useful for qualitative understanding of the phenomenon. The purpose of this section is deriving Eq. (4.2.12), which is equivalent to Eq. (4.1.14) in the  $f(R)$  formulation.

As discussed in Subsec. 3.2.2, the action of the  $f(R)$  theory can be rewritten into that of the scalar-tensor theory as

$$S = \frac{1}{2} \int d^4x \sqrt{-g} [(1 + \varphi)R - 2U(\varphi)] + S_M , \quad (4.2.1)$$

where  $U(\varphi)$  is defined as

$$U(\varphi) \equiv \frac{1}{2} [\varphi A(\varphi) - f(A(\varphi))] , \quad (4.2.2)$$

and  $A(\varphi)$  is the solution of the equation

$$f'(A) = \varphi . \quad (4.2.3)$$

Here we assume  $f''(A) \neq 0$  in order for  $A(\varphi)$  to be uniquely determined. The equation of motion for the scalar field  $\varphi$  is

$$3\Box\varphi - A(\varphi) + \varphi A(\varphi) - 2f(A(\varphi)) = T , \quad (4.2.4)$$

By introducing the potential of the scalar field  $V(\varphi)$  by

$$V_{,\varphi} \equiv \frac{1}{3}[A(\varphi) - \varphi A(\varphi) + 2f(A(\varphi))] , \quad (4.2.5)$$

we can rewrite the equation of motion for  $\varphi$  as

$$\Box\varphi - V_{,\varphi} = \frac{T}{3} . \quad (4.2.6)$$

Assuming  $f(A) \ll A$  and  $\varphi = f'(A) \ll 1$  as before, the derivative of the potential  $V_{,\varphi}$  is approximated as

$$V_{,\varphi} \simeq \frac{A(\varphi)}{3} . \quad (4.2.7)$$

Hereafter we will use this approximate form for  $V_{,\varphi}$ . Though we only need to know  $V_{,\varphi}$  for the following purpose, we can evaluate  $V(\varphi)$  as follows:

$$V(\varphi) = \int d\varphi V_{,\varphi} \simeq \frac{1}{3} \int dA \frac{A}{A_{,\varphi}} = \frac{1}{3} \int dA f''(A)A = \frac{1}{3}[f'(A)A - f(A)] , \quad (4.2.8)$$

where we used the relation  $1/A_{,\varphi} = f''(A)$  obtained by differentiating Eq. (4.2.3) with respect to  $\varphi$ .

Then we consider ultralight scalar field dark matter as the source term in Eq. (4.2.6). Substituting the trace of the energy-momentum tensor of ultralight scalar field dark matter (4.1.5) into Eq. (4.2.6) and assuming  $\Box\varphi \simeq -\ddot{\varphi}$ , the equation of motion for  $\varphi$  can be written as

$$\ddot{\varphi} + V_{,\varphi} = \frac{\rho_0}{3}[1 + 3\cos(2mt)] . \quad (4.2.9)$$

Let us introduce the effective potential  $V_{\text{eff}}(\varphi)$  by

$$V_{\text{eff},\varphi} \equiv V_{,\varphi} - \frac{\rho_0}{3} = \frac{1}{3}[A(\varphi) - \rho_0] . \quad (4.2.10)$$

Note that the effective potential has a minimum at  $R = A(\varphi) = \rho_0$  as desired. Using the effective potential, the equation of motion is written in a simple form:

$$\ddot{\varphi} + V_{\text{eff},\varphi} = \rho_0 \cos(2mt) . \quad (4.2.11)$$

This is the equation of motion for the forced oscillator, which can be analysed with knowledge of classical mechanics. Using the fact that  $\varphi = f_R$ , the formula for calculating the oscillating part of the gravitational potential (4.1.14) can be rewritten in terms of the scalar field  $\varphi$  as

$$\delta\Phi = \delta\Phi_{\text{GR}} \cos(2mt) + \frac{1}{2}(\varphi - \langle\varphi\rangle) , \quad (4.2.12)$$

where we defined  $\delta\Phi_{\text{GR}} \equiv \rho_0/8m^2$ .

Therefore, we have obtained the procedure for calculating the time-dependent part of the gravitational potential in the scalar-tensor formulation as follows: We first calculate the effective potential from a function  $f(R)$  by using Eq. (4.2.10). Then we solve the equation of motion (4.2.11). Finally we substitute the solution into the formula (4.2.12).

# Chapter 5

## Ultralight Scalar Field Dark Matter in $f(R)$ Theory II: Models

In the previous chapter, we have derived the formula, Eq. (4.1.14) or Eq. (4.2.12), for the oscillating part of the gravitational potential induced by the oscillating pressure of ultralight scale field dark matter. We are now in a position to discuss this phenomenon in specific  $f(R)$  models. In this chapter we use the scalar-tensor formalism discussed in Sec. 4.2.

As discussed in Chap. 3, one of the motivations for considering the  $f(R)$  theory of gravity is its ability to resolve the dark energy problem. However we start Sec. 5.1 with the simplest quadratic model  $f(R) \propto R^2$ , which cannot explain dark energy. This is because this model can be solved analytically, and is useful for qualitative understanding of the physics. In studying this model, we do not consider any constraints on the  $f(R)$  theory. We then study the exponential model, in which a function  $f(R)$  depends exponentially on  $R$ , in Sec. 5.2. This is a bit realistic modified gravity model in the sense that the model can pass the local gravity constraint, but we still need a modification for explaining dark energy. By studying this model, we learn a new phenomenon, which is absent in the quadratic model. In Sec. 5.3 we study well-known cosmological dark energy models, which can explain dark energy and at the same time pass the local gravity constraints. This chapter is based on Ref. 19 and Ref. 32.

### 5.1 Quadratic Model

In this section we study the simplest model

$$f(R) = \frac{R^2}{6M^2} , \quad (5.1.1)$$

where  $M$  is a constant with mass dimension one. We study this as a toy model, that is, we do not try to resolve the dark energy problem by this model. The scalaron field  $\varphi$  is defined as

$$\varphi = f'(A) = \frac{A}{3M^2} , \quad (5.1.2)$$

where  $A$  is an auxiliary field. Hence  $A$  is solved as

$$A = 3M^2\varphi . \quad (5.1.3)$$

Using Eq. (4.2.10), the effective potential of the scalaron field  $\varphi$  is calculated as

$$V_{\text{eff}}(\varphi) = \frac{1}{2}M^2(\varphi - \varphi_0)^2 , \quad (5.1.4)$$

where  $\varphi_0 \equiv f'(\rho_0) = \rho_0/3M^2$ . Hence the mass scale  $M$  is nothing but the mass of the scalaron field  $\varphi$  in this model. The equation of motion for the scalaron field  $\varphi$  is

$$\ddot{\varphi} + M^2(\varphi - \varphi_0) = \rho_0 \cos(2mt) . \quad (5.1.5)$$

An important feature of this model is the linearity of the equation of motion for  $\varphi$ . In more general models there is a nonlinear term due to nonlinearity of a function  $A(\varphi)$ , as we will see in the subsequent sections. An induced solution to Eq. (5.1.5) is

$$\varphi = \varphi_0 + \frac{\rho_0}{M^2 - (2m)^2} \cos(2mt) . \quad (5.1.6)$$

Note that we omitted the homogeneous solutions. This is in part because the homogeneous solutions decay in the expanding universe by the Hubble friction, and we expect that only the induced solution remains in the present universe. Since the time-average value of  $\varphi$  is  $\langle \varphi \rangle = \varphi_0$ , the formula (4.2.12) for the oscillating part of the gravitational potential gives

$$\delta\Phi = \frac{\delta\Phi_{\text{GR}}}{1 - (2m/M)^2} \cos(2mt) . \quad (5.1.7)$$

Hence the amplitude of the gravitational potential in the quadratic model  $\delta\Phi_{\text{Quad}}$  is modified relative to that in general relativity  $\delta\Phi_{\text{GR}}$  as

$$\delta\Phi_{\text{Quad}} = \frac{1}{|1 - \mu^2|} \delta\Phi_{\text{GR}} , \quad (5.1.8)$$

where we introduced a dimensionless parameter  $\mu$  as

$$\mu \equiv \frac{2m}{M} . \quad (5.1.9)$$

The amplitude of the oscillating gravitational potential (5.1.8) is plotted in Fig. 5.1. When  $\mu \ll 1$ , the amplitude becomes  $\delta\Phi_{\text{Quad}} \simeq \delta\Phi_{\text{GR}}$ , and the result in Einstein's theory is recovered. This is understood by the fact that when the frequency of the external force  $2m$  is much lower than the intrinsic frequency  $M$ , the system behaves freely under the external force as in Einstein's theory. In the opposite case  $\mu \gg 1$ , the amplitude is suppressed as  $\delta\Phi_{\text{Quad}} \simeq (1/\mu^2)\delta\Phi_{\text{GR}}$ . This is because when the frequency  $2m$  is much higher than the intrinsic frequency  $M$ , the oscillation cannot be excited. The most interesting situation is  $\mu \simeq 1$ . If two mass scales  $M$  and  $2m$  are sufficiently close to each other, resonance would occur and the gravitational potential could be amplified. In this case, the detectability of the oscillating gravitational potential would increase. Of course, the behavior near the resonance point should depend strongly on the details of models. To see this, we study another model in the next section.

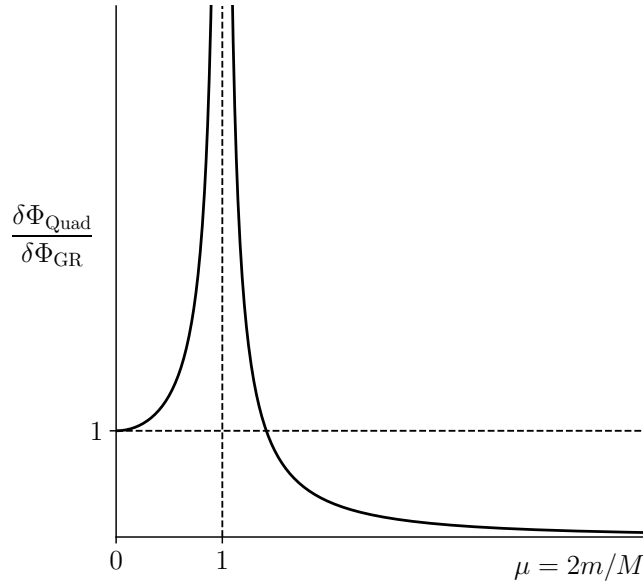


Figure 5.1: The amplitude of the oscillating part of the gravitational potential  $\delta\Phi_{\text{Quad}}$  in the quadratic model (5.1.8), normalized by the value  $\delta\Phi_{\text{GR}}$  in general relativity. This figure is reproduced from Fig. 1 of Ref. 19. (Note that the horizontal axis is inverted.)

## 5.2 Exponential Model

In the previous section we studied the quadratic model, which can be solved analytically. The quadratic model is special in the sense that the equation of motion for the scalaron field  $\varphi$  is linear. However, for general  $f(R)$  models, the equation of motion for  $\varphi$  becomes nonlinear. In this section we investigate an exponential-type model for an example of models with a nonlinear equation of motion for  $\varphi$ .

Let us consider the following model:

$$f(R) = \frac{R_0^2}{3\lambda^2 M^2} \exp \left[ -\lambda \left( \frac{R}{R_0} - 1 \right) \right], \quad (5.2.1)$$

where  $M$  is a constant with mass dimension one, and  $\lambda$  is a positive dimensionless parameter. Although this model looks complicated, we have only one criterion to write down the model: The mass scale of the model should be  $M$  at  $R = R_0$ , i.e.,  $M^2 = 1/3f''(R_0)$ . The effective potential for the scalaron  $\varphi$  is calculated as

$$V_{\text{eff}}(\varphi) = \frac{R_0}{3\lambda} \varphi \left[ 1 - \ln \left( -\frac{3\lambda M^2 \varphi}{R_0} \right) \right] = -M^2 \varphi_0^2 \cdot \frac{\varphi}{\varphi_0} \left[ 1 - \ln \left( \frac{\varphi}{\varphi_0} \right) \right], \quad (5.2.2)$$

where  $\varphi_0$  is the field value at the minimum of the effective potential:

$$\varphi_0 \equiv f'(R_0) = -\frac{R_0}{3\lambda M^2}. \quad (5.2.3)$$

The effective potential (5.2.2) is plotted in Fig. 5.2. The effective potential has a singularity at  $\varphi = 0$ . The gradient of the effective potential,

$$V_{\text{eff},\varphi} = M^2\varphi_0 \ln\left(\frac{\varphi}{\varphi_0}\right), \quad (5.2.4)$$

diverges at this point. Since  $\varphi \rightarrow +0$  corresponds to  $R = A(\varphi) = 3V_{,\varphi} \rightarrow +\infty$ , this point is called the curvature singularity, which often appears in  $f(R)$  models. We can always remove the curvature singularity without affecting the dynamics on the scale we are interested in by adding a regularization term, e.g.,  $R^2/6\mathcal{M}^2$  with a large  $\mathcal{M}$ . However we will not discuss the regularization and just focus on what the exponential model (5.2.1) predicts.

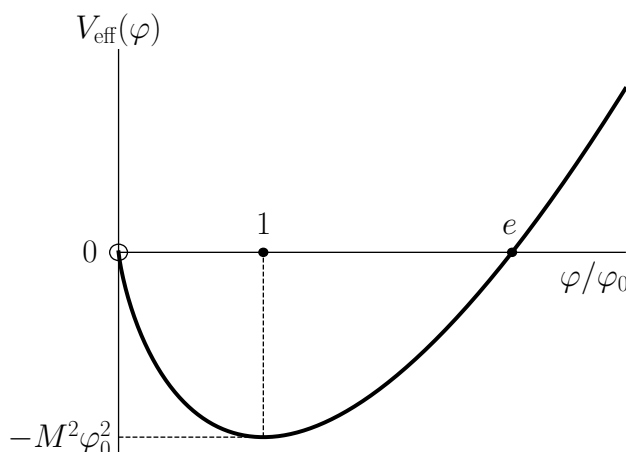


Figure 5.2: The effective potential  $V_{\text{eff}}(\varphi)$  for the scalaron field  $\varphi$  in the exponential model, Eq. (5.2.2). The effective potential has a minimum value  $-M^2\varphi_0^2$  at  $\varphi = \varphi_0$ . The point  $\varphi = 0$  is a singularity, where the gradient of the effective potential diverges. This figure is reproduced from Fig. 1 of Ref. 32.

Let us investigate the equation of motion for the scalaron field

$$\ddot{\varphi} + V_{\text{eff},\varphi} = \rho_0 \cos(2mt), \quad (5.2.5)$$

where the gradient of the effective potential  $V_{\text{eff},\varphi}$  is given by Eq. (5.2.4). In this model the range in which the scalaron field can move over is practically restricted as

$$0 < \varphi/\varphi_0 \lesssim e. \quad (5.2.6)$$

This is because if we start with  $V_{\text{eff}}(\varphi) > 0$ , i.e.,  $\varphi/\varphi_0 > e$ , the scalaron field easily hits the curvature singularity at  $\varphi = 0$ . Hence the possible amplitude of the scalaron field is roughly limited to  $(e/2)|\varphi_0| \sim |\varphi_0|$ , and the maximum amplitude of the gravitational potential is evaluated as

$$\delta\Phi_{\text{max}} \sim \frac{1}{2}|\varphi_0| = \frac{R_0}{6\lambda M^2} \sim \frac{1}{\lambda} \times 10^{-17} \left(\frac{10^{-22} \text{ eV}}{M}\right)^2, \quad (5.2.7)$$

where we assumed the second term in Eq. (4.2.12) is dominant. If the parameter  $\lambda$  is sufficiently small, the oscillating gravitational potential could be large enough to be detected by future experiments.

In the following, we will show that a solution with the maximum amplitude (5.2.7) does exist. For this purpose, let us introduce the dimensionless quantities  $\tau = Mt$ ,  $\mu = 2m/M$ , and  $\bar{\varphi} = \varphi/\varphi_0$ . With these quantities we can rewrite the equation of motion for the scalaron field (5.2.5) as

$$\bar{\varphi}'' + \ln \bar{\varphi} = -3\lambda \cos(\mu\tau) , \quad (5.2.8)$$

where the prime denotes derivative with respect to  $\tau$ . For a linear forced oscillator, the general solution is given by the superposition of an induced solution and the homogeneous solutions. However, for a nonlinear forced oscillator, the superposition of two solutions no longer gives a solution to the equation. Therefore, it is hard to solve a nonlinear system analytically, and we have to rely on a perturbative method or numerical calculations.

### 5.2.1 Perturbative Approach

In order to get an intuition, we first use a perturbative method. We define  $\chi$  as the deviation of  $\bar{\varphi}$  from its minimum value  $\bar{\varphi} = 1$ :

$$\chi \equiv \bar{\varphi} - 1 . \quad (5.2.9)$$

When  $\chi \ll 1$ , we can approximate Eq. (5.2.8) by

$$\chi'' + \chi - \frac{1}{2}\chi^2 + \frac{1}{3}\chi^3 = -3\lambda \cos(\mu\tau) . \quad (5.2.10)$$

This equation can be analyzed perturbatively. Let us seek a resonant solution around  $\mu \sim 1$ . To this aim, we rewrite Eq. (5.2.10) as

$$\chi'' + \mu^2\chi = (\mu^2 - 1)\chi + \frac{1}{2}\chi^2 - \frac{1}{3}\chi^3 - 3\lambda \cos(\mu\tau) . \quad (5.2.11)$$

We regard the terms on the right-hand side as small perturbations. Let us write  $\chi$  as the following series expansion

$$\chi = \chi_0 + \chi_1 + \cdots . \quad (5.2.12)$$

Substituting the series into Eq. (5.2.11), we obtain the lowest order solution

$$\chi_0 = A \cos(\mu\tau) , \quad (5.2.13)$$

where  $A$  is an arbitrary constant. At the next order, we have secular sources

$$\begin{aligned} \chi_1'' + \mu^2\chi_1 &= (\mu^2 - 1)\chi_0 + \frac{1}{2}\chi_0^2 - \frac{1}{3}\chi_0^3 - 3\lambda \cos(\mu\tau) \\ &= \left[ (\mu^2 - 1)A - \frac{1}{4}A^3 - 3\lambda \right] \cos(\mu\tau) + \cdots . \end{aligned} \quad (5.2.14)$$

If this secular term remains, we have a secular solution with a growing amplitude. In other words, we have to renormalize this secular evolution into the frequency. This can be achieved by setting the coefficient of  $\cos(\mu\tau)$  in Eq. (5.2.14) to zero, that is,

$$(A^2 - 4\mu^2 + 4)A = -12\lambda. \quad (5.2.15)$$

Apparently, this allows an order one solution  $A \simeq 2\sqrt{\mu^2 - 1}$  for  $\mu \geq 1$  and  $\lambda \ll 1$ . Thus, we have shown that there exists a resonant oscillation with the amplitude close to the maximum one. As we will see later, we have other resonant solutions at  $\mu = p/q$  with arbitrary positive integers  $p$  and  $q$ . In principle, we can repeat the same analysis to such resonant solutions.

## 5.2.2 Numerical Approach

Next, we investigate the same system numerically. We seek periodic solutions satisfying the periodic condition

$$(\bar{\varphi}(T), \bar{\varphi}'(T)) = (\bar{\varphi}(0), \bar{\varphi}'(0)), \quad (5.2.16)$$

where  $T \equiv 2\pi/\mu$  is the period of the oscillating external force. In other words, we look for solutions with closed orbit in the phase space  $(\bar{\varphi}, \bar{\varphi}')$ . Note that in the quadratic model, this condition removes homogeneous solutions. In order to find such solutions, in general, we should study the map  $(\bar{\varphi}(0), \bar{\varphi}'(0)) \mapsto (\bar{\varphi}(T), \bar{\varphi}'(T))$  and find its fixed points. However, in this case we can perform simpler analysis as follows. The equation of motion (5.2.8) has the time translation symmetry  $t \rightarrow t + T$ . Moreover the system also has time reflection symmetry  $t \rightarrow -t$  thanks to the absence of a friction term. Thus the orbit is closed if  $\bar{\varphi}'(T/2) = 0$  when starting with the initial condition  $(\bar{\varphi}(0), \bar{\varphi}'(0)) = (\bar{\varphi}_i, 0)$ . We should note that the reverse statement is not always true; there exist periodic solutions not satisfying  $\bar{\varphi}'(T/2) = 0$  as we will see later. Hence all we have to do to find periodic solutions is calculating the value  $\bar{\varphi}'(T/2)$  for various initial position  $\bar{\varphi}_i$  and finding its zeros.

We calculate the value  $\bar{\varphi}'(T/2)$  as a function of  $(\mu, \bar{\varphi}_i)$  for different values of  $\lambda$ , and the result is shown in Fig. 5.3. The parameter  $\lambda$  is chosen to be  $\lambda = 10^{-2}, 10^{-3}$ , and  $10^{-4}$ . The red (blue) regions in Fig. 5.3 correspond to positive (negative) values of  $\bar{\varphi}'(T/2)$ . Since  $\bar{\varphi}'(T/2)$  is a smooth function of  $(\mu, \bar{\varphi}_i)$ , there are boundaries with  $\bar{\varphi}'(T/2) = 0$  between two regions (seen as white lines), which correspond to closed-orbit solutions. Hence these plots shows that solutions with amplitude  $|\bar{\varphi}| = |\varphi/\varphi_0| \sim \mathcal{O}(1)$  do exist around  $\mu \sim 1$ . Fig. 5.3 also shows that there are three solutions around  $\mu \gtrsim 1$ . This result has been already suggested in the previous subsection. That is, these solutions are understood as three roots of Eq. (5.2.15). Hence we have confirmed this result again in nonlinear regime, where  $|\bar{\varphi}| \sim \mathcal{O}(1)$ . This is a well-known feature of a nonlinear forced oscillator. For details see standard textbooks of classical mechanics, e.g., Ref. 33.

From Fig. 5.3, we can extract the resonance curves in the following way. For each zero of  $\bar{\varphi}'(T/2)$ , which is on the white lines in Fig. 5.3, we calculate the value  $\delta\varphi \equiv [\varphi(T/2) - \varphi(0)]/2$ . Then we can calculate the the amplitude of the gravitational potential in the

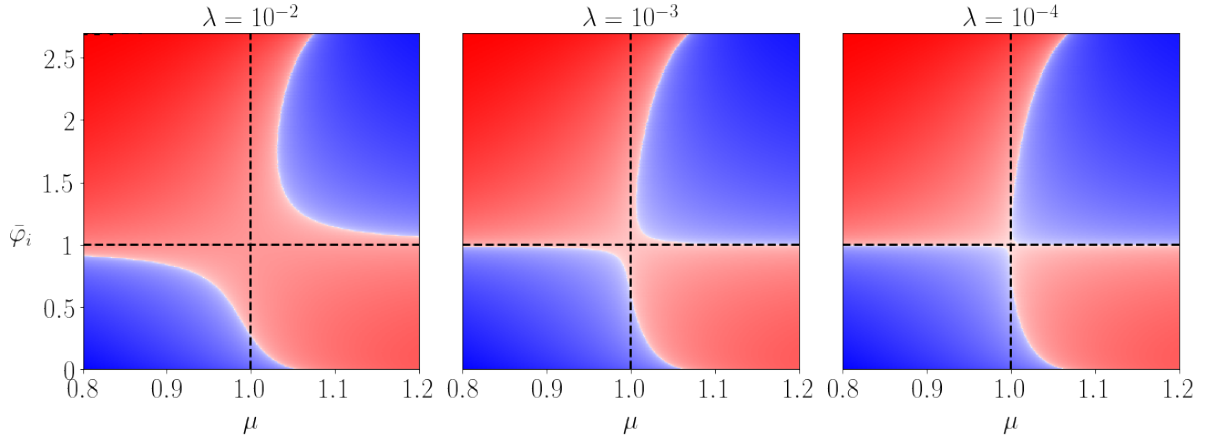


Figure 5.3: The value of  $\bar{\varphi}'(T/2)$  is calculated as a function of  $(\mu, \bar{\varphi}_i)$  for  $\lambda = 10^{-2}, 10^{-3}, 10^{-4}$ . The red (blue) regions correspond to positive (negative) value of  $\bar{\varphi}'(T/2)$ . Since  $\bar{\varphi}'(T/2)$  is a smooth function of  $(\mu, \bar{\varphi}_i)$ , there exist the boundaries with  $\bar{\varphi}'(T/2) = 0$  (white lines), which correspond to closed-orbit solutions. Note that the vertical axes are common in all plots. This figure is reproduced from Fig. 2 of Ref. 32.

exponential model  $\delta\Phi_{\text{Exp}}$  as

$$\delta\Phi_{\text{Exp}} \equiv \frac{1}{2} |\delta\Phi(T/2) - \delta\Phi(0)| = \left| \delta\Phi_{\text{GR}} - \frac{1}{2}\delta\varphi \right|, \quad (5.2.17)$$

where we used Eq. (4.2.12). Using the dimensionless quantity  $\bar{\varphi}$ , we obtain

$$\frac{\delta\Phi_{\text{Exp}}}{\delta\Phi_{\text{GR}}} = \left| 1 + \frac{1}{2}\delta\bar{\varphi} \cdot \frac{|\varphi_0|}{\delta\Phi_{\text{GR}}} \right| = \left| 1 + \frac{\mu^2}{3\lambda}\delta\bar{\varphi} \right|, \quad (5.2.18)$$

where we used the following relation

$$\frac{|\varphi_0|}{\delta\Phi_{\text{GR}}} = \frac{R_0}{3\lambda M^2} \cdot \frac{8m^2}{\rho_0} = \frac{2}{3\lambda} \left( \frac{2m}{M} \right)^2 = \frac{2\mu^2}{3\lambda}. \quad (5.2.19)$$

The resonance curves are plotted in Fig. 5.4. We also plot the resonance curve in the quadratic model for reference. The resonance curves in the exponential model are bent due to nonlinearity of the equation of motion compared to the quadratic case. However, the curves cannot be distinguished from that in the quadratic model except for  $\mu \sim 1$ . Hence we can understand most of the features of this phenomenon from the quadratic model as desired, while the behavior near the resonance point is strongly dependent on the details of models. The maximum amplitude is inversely proportional to  $\lambda$  as seen in Eq. (5.2.7). Note that the discontinuity of the curve seen in the case  $\lambda = 10^{-2}$  comes from the absence of a friction term, as in the case of the quadratic model.

Remarkably, in the nonlinear case such as the exponential model, there appear new resonances at  $\mu = q/p$  for positive integers  $p$  and  $q$  [33]. For an example, we show the same

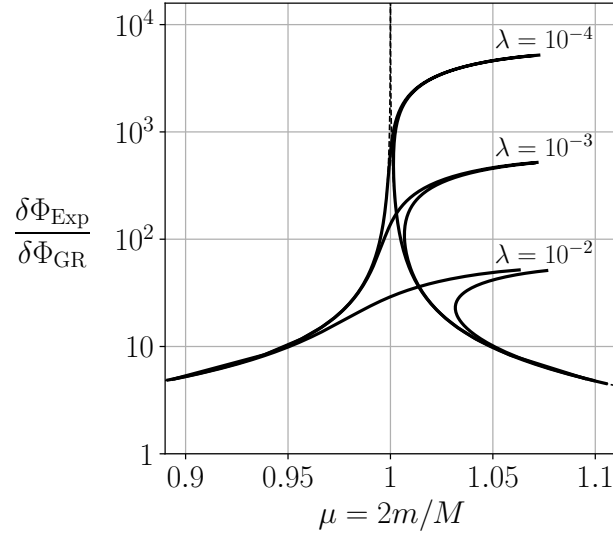


Figure 5.4: The resonance curves around  $\mu = 1$  in the exponential model for  $\lambda = 10^{-2}, 10^{-3}, 10^{-4}$ . The dashed line is the resonance curve in the quadratic model, Eq. (5.1.8). This figure is reproduced from Fig. 3 of Ref. 32.

plot as Fig. 5.3 for the series with  $p = 5$  in Fig. 5.5, where we chose  $\lambda = 10^{-3}$ . Note that the plotted function  $\bar{\varphi}'(T/2)$  is replaced by  $\bar{\varphi}'(5T/2)$  in Fig. 5.5. In these cases, the resonance of the oscillation of the scalaron field occurs when the relation  $M \sim 2m(p/q)$  holds. Hence, the observed frequency becomes both higher or lower than  $2m$ . In the former cases, the frequencies could be accessible by ground-based gravitational-wave detectors such as the LIGO.

### 5.2.3 Constraint on Exponential Model

Before closing the section, let us discuss observational constraints on the exponential model. Following the discussion in Subsec. 3.3.1, the solar system constraint for this model is

$$|\varphi_0| = \frac{3 \times 10^{-18}}{\lambda} \left( \frac{2 \times 10^{-22} \text{ eV}}{M} \right)^2 < 3 \times 10^{-15}. \quad (5.2.20)$$

Hence, the model can pass the solar system test even when  $M = 2 \times 10^{-22} \text{ eV}$  if  $\lambda > 10^{-3}$ . Of course, the larger the mass scale  $M$  is, the easier the model passes the solar system test. Thus the amplitude of the gravitational potential can become as large as  $\delta\Phi_{\text{max}} \simeq 1.5 \times 10^{-15}$ .

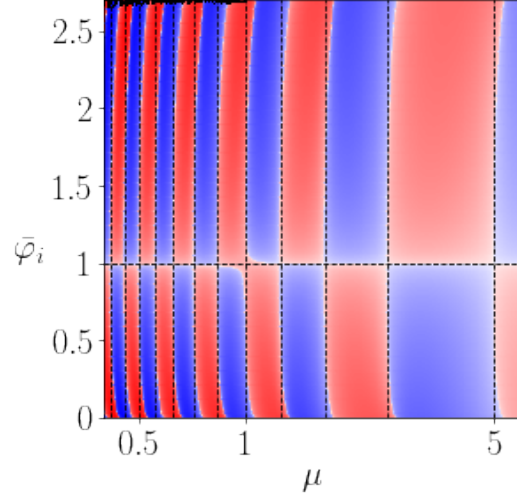


Figure 5.5: The same plot as Fig. 5.3 for the series with  $p = 5$  for  $\lambda = 10^{-3}$ . The plotted function  $\bar{\varphi}'(T/2)$  is replaced by  $\bar{\varphi}'(5T/2)$ . The resonance points correspond to  $\mu = 5/q$  ( $q = 1, 2, 3, \dots$ ). This figure is reproduced from Fig. 4 of Ref. 32.

### 5.3 Cosmological Dark Energy Models

As explained in Sec. 3.1, one of the motivations for modified gravity theories is its ability to resolve the dark energy problem. In the previous two sections, however, we have considered the models that do not explain dark energy. In this section we investigate the behavior of the scalaron field in cosmologically viable  $f(R)$  models, which can explain late time acceleration of the universe. Among a number of proposed models, we here focus on two models known as Hu-Sawicki model [34] and the Starobinsky model [35]. The Hu-Sawicki model  $f_{\text{HS}}(R)$  and the Starobinsky model  $f_{\text{S}}(R)$  are defined as

$$f_{\text{HS}}(R) = -\lambda R_c \frac{(R/R_c)^{2n}}{(R/R_c)^{2n} + 1}, \quad (5.3.1)$$

$$f_{\text{S}}(R) = -\lambda R_c \left[ 1 - \left( 1 + \frac{R^2}{R_c^2} \right)^{-n} \right], \quad (5.3.2)$$

where  $n$  and  $\lambda$  are positive dimensionless parameters, and  $R_c$  is a parameter with the dimension of curvature. In these models,  $f(R)$  vanishes at  $R = 0$  and goes to a constant value  $\lambda R_c$  for  $R \rightarrow +\infty$ . Hence in order for these models to mimic the  $\Lambda$ CDM model, we have to choose  $\lambda R_c \simeq 2\Lambda$ , where  $\Lambda$  is the cosmological constant. Hereafter we assume the relation  $\lambda R_c = 2\Lambda$ , and regard  $n$  and  $\lambda$  as model parameters. The functions  $f_{\text{HS}}(R)$  and  $f_{\text{S}}(R)$  are plotted in Fig. 5.6. When the curvature is large ( $R/R_c \gg 1$ ) both functions have the same asymptotic form:

$$f(R) \simeq -\lambda R_c \left[ 1 - \left( \frac{R}{R_c} \right)^{-2n} \right]. \quad (5.3.3)$$

Since the curvature in the dark matter halo ( $\sim \rho_0$ ) is much larger than the cosmological one ( $\sim R_c$ ), we can use the asymptotic form (5.3.3) for both models when discussing halo scale phenomena.

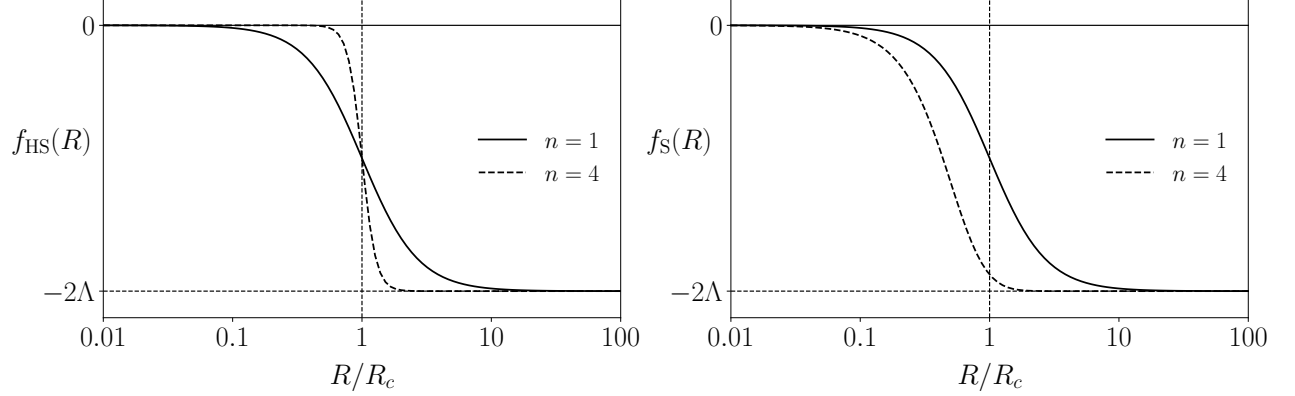


Figure 5.6: The function  $f(R)$  in the Hu-Sawicki model (left) and the Starobinsky model (right). The cases  $n = 1$  and  $n = 4$  are plotted for examples. Note that the relation  $\lambda R_c = 2\Lambda$  is assumed.

### 5.3.1 Effective Potential of Scalaron Field

As mentioned above, we can assume  $R/R_c \gg 1$  in the dark matter halo, and can use the approximated form Eq. (5.3.3) for  $f(R)$ . The auxiliary function  $A(\varphi)$  is defined by

$$\varphi = f'(A) = -2n\lambda \left( \frac{A}{R_c} \right)^{-2n-1}. \quad (5.3.4)$$

Hence we obtain

$$A(\varphi) = R_c \left( \frac{-\varphi}{2n\lambda} \right)^{-1/(2n+1)}. \quad (5.3.5)$$

Note that the scalaron field  $\varphi$  is negative since the function  $f'(R)$  is always negative in this model. We also note that the limit  $\varphi \rightarrow -0$  corresponds to  $A \rightarrow \infty$ . Hence this model also has the curvature singularity at  $\varphi = 0$ . Let us introduce  $\varphi_0 (< 0)$  by

$$\varphi_0 = f'(\rho_0) = -2n\lambda \left( \frac{\rho_0}{R_c} \right)^{-2n-1}. \quad (5.3.6)$$

Then the function  $A(\varphi)$  can be rewritten as

$$A(\varphi) = \rho_0 \left( \frac{\varphi}{\varphi_0} \right)^{-1/(2n+1)}. \quad (5.3.7)$$

The gradient of the effective potential is

$$V_{\text{eff},\varphi} = \frac{1}{3}[A(\varphi) - \rho_0] = \frac{\rho_0}{3} \left[ \left( \frac{\varphi}{\varphi_0} \right)^{-1/(2n+1)} - 1 \right]. \quad (5.3.8)$$

The second derivative of  $V_{\text{eff}}(\varphi)$  is thus

$$V_{\text{eff},\varphi\varphi} = -\frac{\rho_0}{3(2n+1)\varphi_0} \left( \frac{\varphi}{\varphi_0} \right)^{-2(n+1)/(2n+1)}. \quad (5.3.9)$$

Hence the mass scale of the model is

$$M^2 = V_{\text{eff},\varphi\varphi}(\varphi_0) = -\frac{\rho_0}{3(2n+1)\varphi_0} = \frac{\rho_0}{6n(2n+1)\lambda} \left( \frac{\rho_0}{R_c} \right)^{2n+1}. \quad (5.3.10)$$

Integrating Eq. (5.3.8), we obtain the effective potential

$$V_{\text{eff}}(\varphi) = -(2n+1)\varphi_0^2 M^2 \left[ \frac{2n+1}{2n} \left( \frac{\varphi}{\varphi_0} \right)^{2n/(2n+1)} - \frac{\varphi}{\varphi_0} \right], \quad (5.3.11)$$

where we used the definition of the mass (5.3.10). The effective potential is plotted in Fig. 5.7. Note that the points at which  $V_{\text{eff}}(\varphi) = 0$  are  $\varphi = 0$  and

$$\varphi = \left( \frac{2n}{2n+1} \right)^{-2n-1} \varphi_0. \quad (5.3.12)$$

The form of the effective potential seems qualitatively the same as that in the exponential model plotted in Fig. 5.2.

### 5.3.2 Constraints on Hu-Sawicki/Starobinsky model

Before investigating the oscillatory behavior, let us discuss the existing constraints on the Hu-Sawicki and Starobinsky model.

**Local Gravity Constraints** As we have seen in Subsec. 3.3.1, the most stringent constraint among several local gravity tests is from the test of the weak equivalence principle in the solar system. The solar system test gives the constraint  $|\varphi_0| < 3.0 \times 10^{-15}$ , where  $\varphi_0$  is defined by Eq. (5.3.6). The condition can be rewritten as

$$\frac{n}{\lambda^{2n}} \left( \frac{2\Lambda}{\rho_0} \right)^{2n+1} < 1.5 \times 10^{-15}. \quad (5.3.13)$$

Using the plausible cosmological parameters  $h = 0.6731$  and  $\Omega_\Lambda = 0.685$  [1], we can evaluate the ratio

$$\frac{2\Lambda}{\rho_0} = \frac{6\Omega_\Lambda H_0^2}{\rho_0} = 2.18 \times 10^{-5}, \quad (5.3.14)$$

where we assumed  $\rho_0 = 0.3 \text{ GeV/cm}^3$ . Hence the solar system constraint leads  $n > \mathcal{O}(1)$  for  $\lambda = 1$ . In Ref. 19 we used  $n \gtrsim 0.9$  for the local gravity constraints, which is given in Sec. 5 of Ref. 23. However in this thesis we use Eq. (5.3.13) for plotting the local gravity constraints.

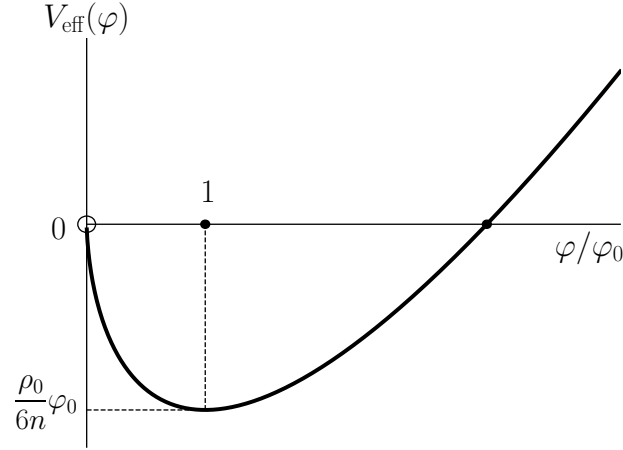


Figure 5.7: The effective potential of the scalaron field in the high-curvature limit of the Hu-Sawicki/Starobinsky model (5.3.11). The point  $\varphi = 0$  is the curvature singularity. Note that  $V_{\text{eff}}(\varphi) = 0$  at  $\varphi = 0$  and  $\varphi/\varphi_0 = [2n/(2n+1)]^{-2n-1}$ .

**Cosmological Constraint** As can be seen in Fig. 5.6, the correction to the  $\Lambda$ CDM model ( $f(R) = -2\Lambda$ ) becomes important around  $R \sim R_c$ . Since the Ricci curvature  $R$  decreases as the universe expands, the larger the value  $R_c$  is, the earlier the time at which the correction becomes important. Thus if  $R_c$  is too large, the model cannot explain cosmological observations such as the CMB. Hence we have an upper bound on  $R_c$ , and equivalently a lower bound on  $\lambda$ , as we fix  $\lambda R_c = 2\Lambda$ . Let us check this explicitly.

With writing the Ricci curvature at the de Sitter point as  $R_{\text{dS}}$ , the condition for the de Sitter point (3.2.5) gives

$$\lambda = \frac{x_{\text{dS}}}{2[1 - (n+1)x_{\text{dS}}^{-2n}]}, \quad (5.3.15)$$

where  $x_{\text{dS}} \equiv R_{\text{dS}}/R_c$ . We can calculate the quantity  $m(r)$  defined by Eq. (3.3.21) as

$$m(r = -2) = -\frac{n(2n+1)\lambda x_{\text{dS}}^{-2n}}{x_{\text{dS}} - \lambda(1 - x_{\text{dS}}^{-2n})} = \frac{n(2n+1)x_{\text{dS}}^{-2n}}{1 - (2n+1)x_{\text{dS}}^{-2n}}, \quad (5.3.16)$$

where we evaluated the value at the de Sitter point ( $r = -2$ ). Hence the stability condition for the de Sitter point,  $0 < m(r = -2) \leq 1$ , reduces to

$$x_{\text{dS}}^{2n} - (n+1)(2n+1) \geq 0, \quad (5.3.17)$$

where we used the condition  $x_{\text{dS}} > 0$ . This inequality can be solved as

$$x_{\text{dS}} \geq [(n+1)(2n+1)]^{1/2n}. \quad (5.3.18)$$

By substituting this into Eq. (5.3.15), we obtain the constraint on the parameter  $\lambda$  for each  $n$ . We use this inequality for the cosmological constraint on the Hu-Sawicki and Starobinsky model.

### 5.3.3 Numerical Approach

The equation of motion for the scalaron field  $\varphi$  is given in Eq. (4.2.11), in which the gradient of the effective potential is given by Eq. (5.3.8). Introducing the dimensionless quantities as before, i.e.,  $\tau = Mt$ ,  $\mu = 2m/M$ , and  $\bar{\varphi} = \varphi/\varphi_0$ , the equation of motion can be rewritten as

$$\bar{\varphi}'' - (2n + 1) [\bar{\varphi}^{-1/(2n+1)} - 1] = -3(2n + 1) \cos(\mu\tau), \quad (5.3.19)$$

where the prime denotes derivative with respect to  $\tau$ . We can repeat the same analysis as in the exponential model, and then obtain a similar plot as Fig. 5.3. In Fig. 5.8, we plot the value of  $\bar{\varphi}'(T/2)$  as a function of  $(\mu, \bar{\varphi}_i)$  for  $n = 1$ . Note that zeros of  $V_{\text{eff}}(\varphi)$  are at  $\varphi = 0$  and  $\varphi/\varphi_0 = 27/8 = 3.375$  for  $n = 1$ . As in Fig. 5.3, the red (blue) region corresponds to positive (negative) value of  $\bar{\varphi}'(T/2)$ . In this model, we have a large unstable region that is shown in black. That is, when we start with a set of parameters  $(\mu, \bar{\varphi}_i)$  in the black region, the scalaron hits the curvature singularity at  $\varphi = 0$ .

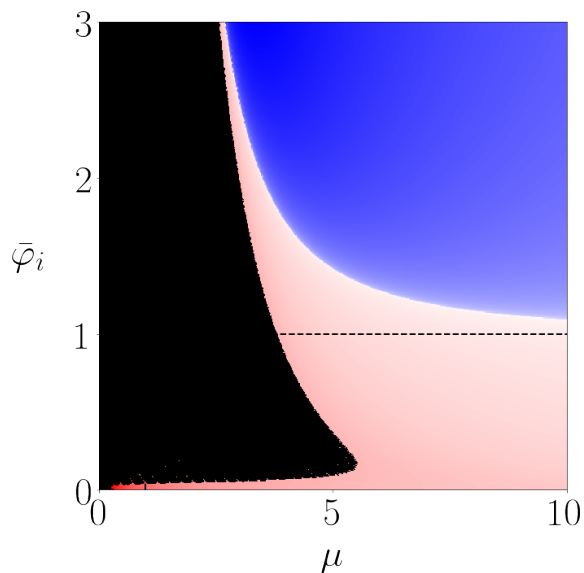


Figure 5.8: The value of  $\bar{\varphi}'(T/2)$  is calculated as a function of  $(\mu, \bar{\varphi}_i)$  for  $n = 1$ . The red (blue) region corresponds to positive (negative) value of  $\bar{\varphi}'(T/2)$ . When starting with a set of parameters  $(\mu, \bar{\varphi}_i)$  in the black region, the scalaron hits the curvature singularity at  $\varphi = 0$ .

Fig. 5.8 shows that there exist solutions with amplitude  $\bar{\varphi} = \mathcal{O}(1)$ , i.e.,  $|\varphi| = \mathcal{O}(|\varphi_0|)$ . Since  $|\varphi_0|$  can be as large as  $|\varphi_0| \sim 3 \times 10^{-15}$  as in the exponential model, we also have resonance solutions in this model. However, there is a large unstable region in this model compared to the exponential model. This is due to the difference of the effective potentials. Hence we need a condition  $\mu = 2m/M \gtrsim \mathcal{O}(1)$  for the stability of the system without a modification of the curvature singularity. This condition is plotted together with the cosmological and local gravity constraints in Fig. 5.8.<sup>1</sup> In Fig. 5.8 the lines  $\mu = 1$  with three

<sup>1</sup> We used the values  $\rho_0 = 0.3 \text{ GeV/cm}^3$ ,  $\Omega_\Lambda = 0.685$ , and  $h = 0.6731$  for numerical calculations. In

different masses are plotted as references of the stability condition. Note that the condition  $\mu > 1$  is slightly weaker than that seen in Fig. 5.8.

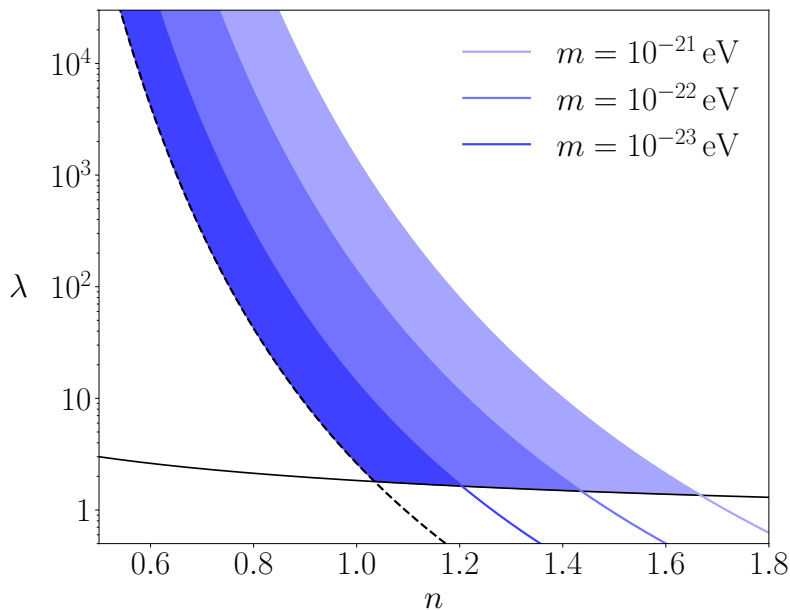


Figure 5.9: The stability conditions are plotted together with the cosmological constraint (black solid line) and local gravity constraint (black dashed line). This figure is reproduced from Fig. 2 of Ref. 19.

In closing the section, let us summarize the behavior of the gravitational potential in the Hu-Sawicki or Starobinsky dark energy model. As in the case of the quadratic model and the exponential model, we have resonance solutions for scalaron field with amplitude of order  $|\varphi_0|$ , which is constrained as  $|\varphi_0| < 3 \times 10^{-15}$  by the solar system tests. Hence the amplitude of the gravitational potential can become as large as  $\delta\Phi_{\max} \sim 1.5 \times 10^{-15}$  under the resonant condition, which could be detected by future experiments. When  $\mu \gg 1$ , the oscillation of the scalaron field is suppressed as in the previous models. However, in the case  $\mu \lesssim \mathcal{O}(1)$ , the instability of the model becomes a problem. In this case the scalaron field easily hits the curvature singularity at  $\varphi = 0$ . Hence in order for the model to be stable and consistent with the existing constraints, the parameters  $(n, \lambda)$  should be constrained in the colored region in Fig. 5.9. Of course, it might be natural to consider a modification for curing the singularity, while this is beyond the scope of this thesis.

---

plotting Fig. 2 in Ref. 19, we missed a factor 0.3 of  $\rho_0 = 0.3 \text{ GeV}/\text{cm}^3$ . Thus three lines for stability are slightly shifted to right relative to those in Fig. 2 in Ref. 19.

# Chapter 6

## Conclusion

In this thesis we have studied a gravitational phenomenon caused by the oscillating pressure of ultralight scalar field dark matter in the framework of the  $f(R)$  theory. The ultralight scalar field dark matter model recently attracts much attention partly because it could resolve the so-called “small scale crisis” of the standard cold dark matter model. The fact that the collider experiments have shown no sign of supersymmetric particles can also be a motivation for considering alternatives to WMIPs.

A phenomenon caused by ultralight scalar field dark matter had been already investigated based on general relativity, and shown that the induced oscillation of the gravitational potential could be detected by future experiments. However, there are some reasons to consider theories of gravity other than general relativity. Hence it is worth investigating the phenomenon in the framework of modified gravity theories.

We have focused on the  $f(R)$  theory in this thesis since it is one of the simplest theories of modified gravity. We have discovered the resonant amplification of the gravitational potential, which is absent in Einstein’s theory. This comes from the fact that the  $f(R)$  theory includes a new dynamical degree of freedom dubbed the scalaron. A wide class of modified gravity theories also include the scalaron field. The dynamics of the scalaron field is excited by the oscillating pressure of ultralight scalar field dark matter. If the angular frequency of the pressure, which is twice as the mass of ultralight scalar field, is sufficiently close to the mass of the scalaron field, the scalaron field is amplified dramatically. Since the gravitational potential is determined by the scalaron field in the  $f(R)$  theory, the gravitational potential is also amplified in that situation. We have also found that the resonance behavior also appears when the fraction of the angular frequency of the pressure and the scalaron mass is close to an arbitrary rational number. If the resonant oscillation is excited, the oscillation of the gravitational potential is expected to be detected by future gravitational experiments.

# Acknowledgement

I would like to thank my supervisor Prof. Soda for fruitful discussions and collaborations. This work was in part supported by JSPS Grant-in-Aid for JSPS Research Fellow Grant No. 17J00568.

# Reference

- [1] P. A. R. Ade *et al.* (Planck Collaboration), “*Planck 2015 results - XIII. Cosmological parameters*,” *A&A* **594**, A13 (2016), arXiv:1502.01589 [astro-ph.CO].
- [2] A. Khmelnitsky and V. Rubakov, “*Pulsar timing signal from ultralight scalar dark matter*,” *JCAP* **02** (2014) 019, arXiv:1309.5888 [astro-ph.CO].
- [3] D. J. E. Marsh, “*Axion cosmology*,” *Phys. Rept.* **643** (2016) 1, arXiv:1510.07633 [astro-ph.CO].
- [4] L. Hui, J. P. Ostriker, S. Tremaine, and E. Witten, “*Ultralight scalars as cosmological dark matter*,” *Phys. Rev. D* **95**, 043541 (2017), arXiv:1610.08297 [astro-ph.CO].
- [5] D. H. Weinberg, J. S. Bullock, F. Governato, R. Kuzio de Naray, and A. H. G. Peter, “*Cold dark matter: Controversies on small scales*,” *Proc. Nat. Acad. Sci.* **112**, 12249 (2015), arXiv:1306.0913 [astro-ph.CO].
- [6] W. Hu, R. Barkana, and A. Gruzinov, “*Fuzzy Cold Dark Matter: The Wave Properties of Ultralight Particles*,” *Phys. Rev. Lett.* **85**, 1158 (2000), arXiv:astro-ph/0003365.
- [7] J.-c. Hwang and H. Noh, “*Axion as a cold dark matter candidate*,” *Phys. Lett. B* **680**, 1 (2009), arXiv:0902.4738 [astro-ph.CO].
- [8] D. Blas, J. Lesgourgues, and T. Tram, “*The Cosmic Linear Anisotropy Solving System (CLASS). Part II: Approximation schemes*,” *JCAP* **07** (2011) 034, arXiv:1104.2933 [astro-ph.CO].
- [9] L. A. Ureña López and A. X. Gonzalez-Morales, “*Towards accurate cosmological predictions for rapidly oscillating scalar fields as dark matter*,” *JCAP* **07** (2016) 048, arXiv:1511.08195 [astro-ph.CO].
- [10] H.-Y. Schive, T. Chiueh, and T. Broadhurst, “*Cosmic structure as the quantum interference of a coherent dark wave*,” *Nat. Phys.* **10**, 496 (2014), arXiv:1406.6586 [astro-ph.GA].
- [11] R. Hlozek, D. Grin, D. J. E. Marsh, and P. G. Ferreira, “*A search for ultralight axions using precision cosmological data*,” *Phys. Rev. D* **91**, 103512 (2015), arXiv:1410.2896 [astro-ph.CO].

- [12] P. A. R. Ade *et al.* (Planck Collaboration), “*Planck 2013 results. XV. CMB power spectra and likelihood*,” *A&A* **571**, A15 (2014), arXiv:1303.5075 [astro-ph.CO].
- [13] R. Hložek, D. J. E. Marsh, D. Grin, R. Allison, J. Dunkley, and E. Calabrese, “*Future CMB tests of dark matter: Ultralight axions and massive neutrinos*,” *Phys. Rev. D* **95**, 123511 (2017), arXiv:1607.08208 [astro-ph.CO].
- [14] R. Hložek, D. J. E. Marsh, and D. Grin, “*Using the full power of the cosmic microwave background to probe axion dark matter*,” *Mon. Not. Roy. Astron. Soc.* **476**, 3063 (2018), arXiv:1708.05681 [astro-ph.CO].
- [15] N. Aghanim *et al.* (Planck Collaboration), “*Planck 2015 results - XI. CMB power spectra, likelihoods, and robustness of parameters*,” *A&A* **594**, A11 (2016), arXiv:1507.02704 [astro-ph.CO].
- [16] V. Iršič, M. Viel, M. G. Haehnelt, J. S. Bolton, and G. D. Becker, “*First Constraints on Fuzzy Dark Matter from Lyman- $\alpha$  Forest Data and Hydrodynamical Simulations*,” *Phys. Rev. Lett.* **119**, 031302 (2017), arXiv:1703.04683 [astro-ph.CO].
- [17] E. Armengaud, N. Palanque-Delabrouille, C. Yèche, D. J. E. Marsh, and J. Baur, “*Constraining the mass of light bosonic dark matter using SDSS Lyman- $\alpha$  forest*,” *Mon. Not. Roy. Astron. Soc.* **471**, 4606 (2017), arXiv:1703.09126 [astro-ph.CO].
- [18] A. Aoki and J. Soda, “*Detecting ultralight axion dark matter wind with laser interferometers*,” *Int. J. Mod. Phys. D* **26**, 1750063 (2016), arXiv:1608.05933 [astro-ph.CO].
- [19] A. Aoki and J. Soda, “*Pulsar timing signal from ultralight axion in  $f(R)$  theory*,” *Phys. Rev. D* **93**, 083503 (2016), arXiv:1601.03904 [hep-ph].
- [20] B. P. Abbott *et al.* (LIGO Scientific Collaboration and Virgo Collaboration), “*Observation of Gravitational Waves from a Binary Black Hole Merger*,” *Phys. Rev. Lett.* **116**, 061102 (2016), arXiv:1602.03837 [gr-qc].
- [21] K. Kuroda, W.-T. Ni, and W.-P. Pan, “*Gravitational waves: Classification, methods of detection, sensitivities and sources*,” *Int. J. Mod. Phys. D* **24**, 1530031 (2015), arXiv:1511.00231 [gr-qc].
- [22] A. A. Starobinsky, “*A new type of isotropic cosmological models without singularity*,” *Phys. Lett. B* **91**, 99 (1980).
- [23] A. De Felice and S. Tsujikawa, “ *$f(R)$  Theories*,” *Living Rev. Rel.* **13** (2010) 3, arXiv:1002.4928 [gr-qc].
- [24] C. Brans and R. H. Dicke, “*Mach’s Principle and a Relativistic Theory of Gravitation*,” *Phys. Rev.* **124**, 925 (1961).
- [25] G. W. Horndeski, “*Second-order scalar-tensor field equations in a four-dimensional space*,” *Int. J. Theor. Phys.* **10**, 363 (1974).

- [26] J. Khoury and A. Weltman, “*Chameleon cosmology*,” Phys. Rev. D **69**, 044026 (2004), arXiv:astro-ph/0309411.
- [27] J. Khoury and A. Weltman, “*Chameleon Fields: Awaiting Surprises for Tests of Gravity in Space*,” Phys. Rev. Lett. **93**, 171104 (2004), arXiv:astro-ph/0309300.
- [28] B. Bertotti, L. Iess, and P. Tortora, “*A test of general relativity using radio links with the Cassini spacecraft*,” Nature **425**, 374 (2003).
- [29] S. Baeßler, B. R. Heckel, E. G. Adelberger, J. H. Gundlach, U. Schmidt, and H. E. Swanson, “*Improved Test of the Equivalence Principle for Gravitational Self-Energy*,” Phys. Rev. Lett. **83**, 3585 (1999).
- [30] L. Amendola, R. Gannouji, D. Polarski, and S. Tsujikawa, “*Conditions for the cosmological viability of  $f(R)$  dark energy models*,” Phys. Rev. D **75**, 083504 (2007), arXiv:gr-qc/0612180.
- [31] B. Abbott *et al.* (LIGO Scientific Collaboration and Virgo Collaboration), “*GW170817: Observation of Gravitational Waves from a Binary Neutron Star Inspiral*,” Phys. Rev. Lett. **119**, 161101 (2017), arXiv:1710.05832 [gr-qc].
- [32] A. Aoki and J. Soda, “*Nonlinear resonant oscillation of gravitational potential induced by ultralight axion in  $f(R)$  gravity*,” Phys. Rev. D **96**, 023534 (2017), arXiv:1703.03589 [astro-ph.CO].
- [33] L. D. Landau and E. M. Lifshitz, “*Mechanics*,” (Pergamon Press, New York, 1960).
- [34] W. Hu and I. Sawicki, “*Models of  $f(R)$  cosmic acceleration that evade solar system tests*,” Phys. Rev. D **76**, 064004 (2007), arXiv:0705.1158 [astro-ph].
- [35] A. A. Starobinsky, “*Disappearing cosmological constant in  $f(R)$  gravity*,” JETP Lett. **86**, 157 (2007), arXiv:0706.2041 [astro-ph].